International Journal of Hydrogen Energy 160 (2025) 150466

Contents lists available at ScienceDirect

International Journal of Hydrogen Energy

journal homepage: www.elsevier.com/locate/he

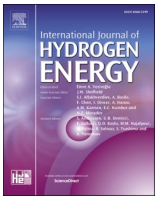

Electrification of catalytic methane decomposition to hydrogen and nanostructured carbonaceous materials

Sergey Girshevich [a,b], David Bajec [a], Stanislav Yakushkin [a], Janvit Teržan [a], Blaž Likozar [a,*]

[a] Department of Catalysis and Chemical Reaction Engineering, National Institute of Chemistry, Hajdrihova 19, SI-1001, Ljubljana, Slovenia
[b] Faculty of Chemistry and Chemical Engineering, University of Maribor, Smetanova ul. 17, SI-2000, Maribor, Slovenia

ARTICLE INFO

Handling Editor: Dr V Palma

Keywords:
Catalytic methane decomposition
Microwave heating
Plasma catalysis
Hydrogen production
Carbon nanotubes
Graphene

ABSTRACT

The catalytic decomposition of methane to produce hydrogen and carbon is an economically and environmentally attractive approach to creating a CO/CO_2-free cycle for hydrogen production. In order to achieve this, it is crucial to use electricity from renewable or alternative energy sources that operate without CO/CO_2 emissions. Currently, however, most developments have not progressed beyond the laboratory level. This paper summarizes the current status and perspectives of the main methods of catalytic methane decomposition electrification. This review provides an outlook on producing nanostructured carbonaceous products, such as carbon nanotubes, nanofibers, graphene, and graphite. By systematically summarizing literature on this topic, we provide a comprehensive, simplified overview of the field, emphasizing catalyst and reactor design, as well as possible routes to the electrification of catalytic methane decomposition, including plasma, microwave, and induction heating.

1. Introduction

According to the International Energy Agency's (IEA) World Energy Outlook, global electricity consumption increased by 590 TWh between 2010 and 2023, rising from 21,851 TWh to 22,442 TWh. The IEA projects that consumption will rise by over 900 TWh between 2023 and 2035 (Fig. 1A). Meanwhile, fossil fuels will account for two-thirds of the increase in electricity demand in 2023 will be met by fossil fuels, driving energy-related CO_2 emissions to a new record high [1]. Continued reliance on fossil fuels as a primary energy source will inevitably lead to increased CO_2 emissions. Rising CO_2 emissions exacerbate the ongoing climate crisis, resulting in serious long-term environmental [2], economic [3] and social [4] consequences. An alternative to this trend is transitioning to energy carriers that do not constantly emit carbon. One candidate for this role is hydrogen [5], the combustion of which produces only water vapor. However, using hydrogen as a fuel presents several challenges, one of which is the cost of production [6]. Currently, the production of hydrogen through water electrolysis is not yet economical, and most of today's hydrogen is produced by cracking natural gas or crude oil, or by methane reforming. The process results in the production of 14 tons of CO_2 for every ton of hydrogen produced. Therefore, there is a need to create an economically viable CO_2-free hydrogen production cycle integrated with renewable energy sources [7]. Although hydrogen is often described as a clean fuel because it produces only water vapor upon combustion or conversion in fuel cells, its environmental value depends critically on the carbon footprint of its production process. Conventional production methods, such as SMR, emit large quantities of CO and CO_2, which undermines its climate benefits. For hydrogen to serve as a genuinely sustainable, climate-neutral energy carrier, production cycles must be completely free of carbon oxides emissions, both in terms of reaction byproducts and the source of process heat. Electrification powered by renewable energy sources offers a promising pathway to achieving this goal.

Today, the main source of hydrogen is methane. In 2019, methane-based processes accounted for 96% of hydrogen production [8,9]. Currently, there are four main methods for obtaining hydrogen from methane: SMR [10] (eq. (1)), dry reforming of methane [11] (eq. (2)), partial oxidation of methane [12] (eq. (3)), and CDM [13] (eq. (4)).

$$CH_4 + H_2O \leftrightarrow CO + 3H_2 \quad (1)$$

$$CH_4 + CO_2 \leftrightarrow 2CO + 2H_2 \quad (2)$$

* Corresponding author.
E-mail addresses: Sergey.Girshevich@ki.si (S. Girshevich), David.Bajec@ki.si (D. Bajec), Stanislav.Iakushkin@ki.si (S. Yakushkin), Janvit.Terzan@ki.si (J. Teržan), Blaz.Likozar@ki.si (B. Likozar).

https://doi.org/10.1016/j.ijhydene.2025.150466
Received 23 January 2025; Received in revised form 4 July 2025; Accepted 10 July 2025
Available online 29 July 2025

List of abbreviations and units

SMR	Steam methane reforming
CDM	Catalytic methane decomposition
CNT	Carbon nanotube
MWCNT	Multiwall carbon nanotube
SWCNT	Single wall nanotube
CNF	Carbon nanofiber
CNO	Carbon nanoonion
AC	Activated carbon
CB	Carbon black
CC	Carbon-carbon
TEM	Transmission electron microscopy
HRTEM	High resolution transmission electron microscopy
FESEM	Field emission scanning electron microscopy
SEM	Scanning electron microscopy
TGA	Thermogravimetric analysis
XRD	X-Ray diffraction
GHSV	Gas hourly space velocity
X_{CH_4}	Methane conversion
SV	Space velocity
VHSV	Volumetric hourly space velocity
TWh	Terawatt hours
Mt	Megaton
MWh_{H_2}	Megawatt-hours, produced by H_2
g_{cat}	Gram of catalyst
atm	Standard atmosphere
sccm	Standard cubic centimeter per minute
FBR	Fixed-bed reactor
FlBR	Fluidized bed reactor
MMBCR	Molten metal bubble column reactor
DBD	Dielectric barrier discharge
TRL	Technology readiness level
n.d.	No data

$$CH_4 + 1/2O_2 \leftrightarrow CO + 2H_2 \quad (3)$$

$$CH_4 \leftrightarrow C + 2H_2 \quad (4)$$

Currently, the most common method of converting methane into hydrogen is SMR. In 2024, approximately 35% (0.6 Mt/year out of 0.9–1.2 Mt/year) of hydrogen was produced by SMR, accounting for over half (0.6 Mt/year) of the hydrogen produced by low-emission technologies [14]. The CDM process is one of the most important alternatives to methane reforming [15]. It requires less energy and does not emit carbon oxides into the atmosphere [16,17]. According to the annual Global Hydrogen Review, CDM shows the greatest readiness growth among all low-emission hydrogen production technologies from 2021 to 2024 (see Fig. 1B and C) [14,18].

Producing hydrogen by CDM is also more economically viable than producing it by SMR. Keipi et al. [19] conducted an economic analysis of various methods of hydrogen production (Fig. 1D). The authors considered the direct carbon dioxide emissions from the reaction and the emissions from providing the reaction with energy. They demonstrated that the specific carbon dioxide emissions for hydrogen production by CDM are $\frac{40kg_{CO_2}}{MWh_{H_2}}$ vs $\frac{133kg_{CO_2}}{MWh_{H_2}}$ for SMR. According to other economic estimates, CDM could be a cost-effective method of producing hydrogen while reducing greenhouse gas emissions [20–22]. Keipi et al. [23] compared different methods of hydrogen production from methane and showed that CDM significantly reduces the carbon footprint compared to SMR. With SMR, 1 L of carbon monoxide is produced for every 3 L of hydrogen, and capturing it requires greater effort.

Musomali and Isa [24] stated that the main direction of further CDM development should be the creation of new, improved commercial catalysts. The main problem hindering the industrial utilization of CDM is catalyst deactivation due to sintering and coking, caused by the formation of solid carbon on the catalyst surface [25]. Currently, the main obstacles to the wider application of CDM lie in the catalysts' various disadvantages, such as their relatively rapid loss of catalytic activity and the need for regular regeneration.

Although improving catalytic performance remains the primary objective of CDM development, other researchers have emphasized the importance of a multidisciplinary approach that encompasses not only the development of new catalytic materials but also economic analysis. For example, Qian et al. [26] conducted an economic evaluation of different CDM processes and demonstrated that operating efficiency is not the only important parameter of a CDM process; the cost of catalyst production is also important. Hydrogen production using inexpensive catalysts with low conversion efficiency can be more economically valuable than using expensive catalysts with high efficiency. For instance, Ni-based catalysts yield more hydrogen than Fe-based catalysts (0.39 mol_{H_2}/g_{cat}/h vs 0.22 mol_{H_2}/g_{cat}/h), yet the cost of hydrogen production using Ni-based catalysts is much higher ($0.89 vs $0.009 for mole of H_2). The economic efficiency of CDM is influenced not only by efficiency parameters, but also by variables such as catalyst cost, reactor design, energy consumption, and catalyst regeneration techniques [22]. Ashik et al. [27] emphasize the use of membranes to separate gases in the outlet stream, which increases the efficiency of the CDM process. Additionally, it has repeatedly been shown that the greatest influence on the economic efficiency of CDM is the price of the carbon produced during the reaction [22,23,28]. The most valuable carbon products are carbon nanotubes (CNTs) [29,30], which are known to form in the CDM process (Fig. 2) [31–35]. Some authors even consider catalytic methane decomposition primarily as a method for producing high-value carbon materials such as graphene and carbon nanotubes, while treating hydrogen as a secondary byproduct [36]. Therefore, searching for catalysts that produce high-value carbon is also a high priority for CDM development.

Another way to improve the economic efficiency of the CDM and reduce its environmental impact is through electrification. Electrification uses electrical energy, as opposed to conventional, fossil fuel–based heat, to provide necessary heat for the CDM. This includes plasma, microwave, and induction heating methods, which can be powered by renewable electricity. Using these techniques, it is possible to achieve completely CO_2-free production of hydrogen in terms of both reaction chemistry and energy input provided that the electricity comes from renewable sources. Electrification can significantly reduce the carbon emissions needed to heat the reaction medium and often circumvents reaction-limiting difficulties. Similar improvements have already been successfully applied to methane reforming [37–39], and changing the heating method affects not only the energy source but also other technical features of the reactor. However, this topic is insufficiently covered with regard to CDM. While individual experiments on CDM electrification have been published, there is no comprehensive overview of the current state and future prospects of this field. Only Kim et al. [38] and Keipi et al. [40] have briefly mentioned this topic. Kim et al.'s review focused on thermochemical catalytic reactions with Joule and induction heating. Their review contains a fairly detailed analysis of the prospects for using Joule and induction heating for thermochemical reactions but does not discuss CDM. Keipi et al. discussed various methods of supplying heat to CDM, including some electrified reactors. However, the main focus of this work was the reaction parameters of CDM. Additionally, nine years have passed since this publication, during which time the number of papers addressing non-conventional methods of

CDM heat supply has grown considerably.

A number of comprehensive review papers have been published that provide broader context for CDM research. Fan et al. [9] offered a historical overview of CDM development, including reaction mechanisms, catalyst systems, and major technological challenges. Alves et al. [13] and Patlola et al. [41] emphasized the commercialization potential and techno-economic barriers facing CDM, with a particular focus on its role in the energy transition. Hanotoko et al. [25] published the most up-to-date and complete general review, covering all major classes of solid catalysts and evaluating their technical and economic viability. Hamdan et al. [42] concentrated on catalyst development pathways, while Qian et al. [43] examined reactor design and the comparative performance of metal-based catalysts across various configurations. In addition to these general reviews, numerous topic-specific reviews have

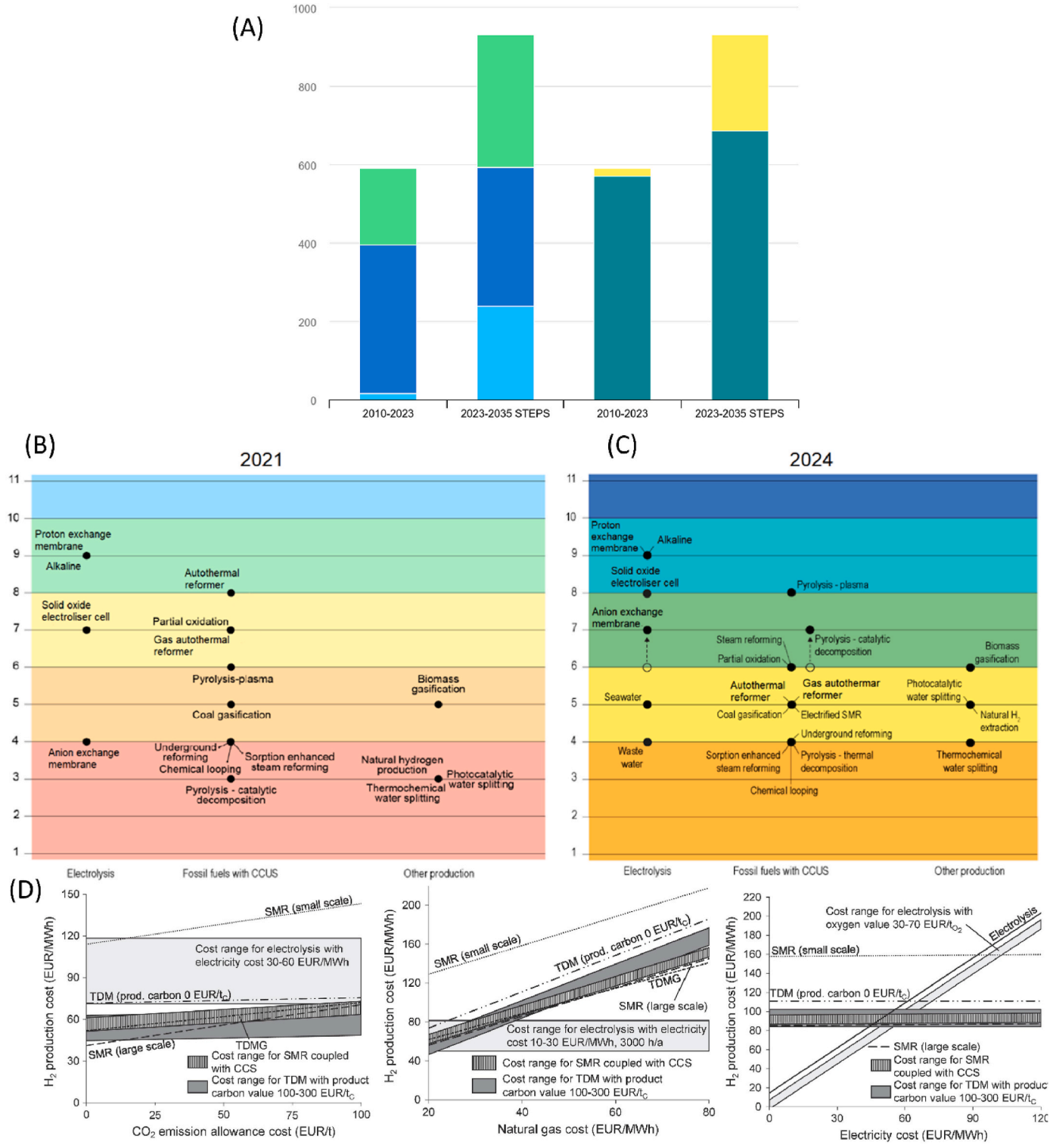

Fig. 1. (A) Historical and projected annual growth in electricity demand from 2010 to 2035 (IEA. Licence: CC BY 4.0) [1]; TRL of production of various low-emission hydrogen production technologies (B) in 2021 (IEA. Licence: CC BY 4.0) [18] and (C) in 2024 (IEA. Licence: CC BY 4.0) 2024 [14]; (D) Cost of hydrogen production using different methods, depending on the cost of CO_2 emissions, natural gas and electricity [19].

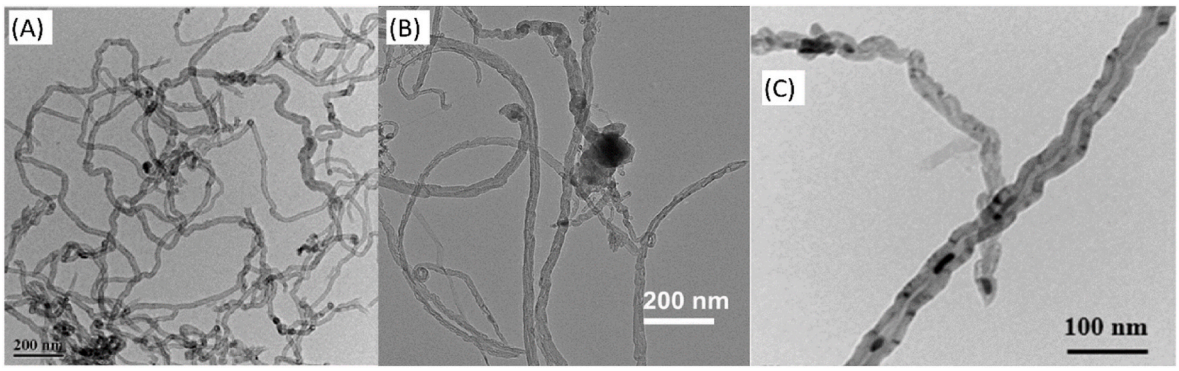

Fig. 2. HRTEM of CNTs produced via CDM using the following catalysts: (A) Ni/MgO [32] (B) $FeCo/Al_2O_3$ (MDPI. Licence: CC BY 4.0) [34] and (C) $Ni/CaTiO_3$ [35].

been published in recent years, each focusing on narrower aspects of CDM or electrification [15,44–66].

However, despite the depth and breadth of these reviews, none provides a dedicated treatment of electrified CDM, which represents an increasingly important strategy for decarbonized hydrogen production.

This paper presents a comprehensive review of electrification strategies for catalytic methane decomposition (CDM) as a sustainable pathway for the co-production of hydrogen and carbon. While covering the fundamentals of CDM—such as reactor configurations, catalyst systems, and carbon product valorization—we place particular emphasis on non-conventional, electricity-driven heating methods, including plasma catalysis, microwave dielectric heating, and induction heating. These electrified approaches offer the potential to decouple methane conversion from fossil fuel–based heat sources, thereby enabling a CO_2-free production cycle when powered by renewable electricity.

In contrast to previous reviews, our work uniquely focuses on electrified CDM, providing a comparative and integrative analysis of plasma, microwave, and induction heating technologies. We examine their underlying mechanisms, reactor integration strategies, technology readiness levels, and implications for the co-production of hydrogen and nanostructured carbon materials. This topical focus is especially timely given the increasing global demand for carbon oxide–free hydrogen production.

To support further research and industrial deployment, we also critically assess the challenges, limitations, and future prospects of each electrification method within the broader context of sustainable energy systems.

2. Catalytic methane decomposition

2.1. Catalysts

The catalytic decomposition of methane (CDM) was first described in 1890 by Schützenberger and Schützenberger [67]. CDM can occur at a temperature of 400°C, making CDM an attractive option economically and ecologically compared to other methods [9,26,68]. Weger et al. [69] assume that CDM has the potential to bridge the gap to a hydrogen economy.

CDM produces hydrogen and various types of carbon, which can have their own economic value. The carbon produced during CDM can be categorized by increasing economic value as follows: carbon black (amorphous carbon), graphite, CNFs, multi-walled carbon nanotubes (MWCNTs), and single-walled carbon nanotubes (SWCNTs). The type of carbon produced mainly depends on the catalyst (Fig. 3A) and the support (Fig. 3B) [24,33,48,65,70–75], but it can also be controlled by reaction conditions such as temperature (Fig. 3D) and gas flow (Fig. 3C) [48,76–79].

A wide range of different catalysts is suitable for CDM. Hantoko et al. [25] provide a detailed discussion of solid CDM catalysts in their review, while McConnachie et al. [66] focus more on molten catalysts. These authors analyzed the strengths and weaknesses of currently available catalysts and their productivity.

This section provides an overview of the main categories of catalysts. Table 1 lists comparative data on examples of the most prominent catalysts reported in the open literature.

2.1.1. Carbon catalysts

As previously mentioned, carbon catalysts were the first CDM catalysts to be tested experimentally, with proof first being provided as early as 1890 [67]. However, these studies are currently only of historical value. Modern researchers [96–98] usually consider Muradov [99–102] a pioneer in the field of carbon catalysts CDM. In his initial publication on the subject in 1998, Muradov demonstrated the competitiveness of carbon catalysts compared to metal oxide catalysts. He also highlighted one of the primary advantages of carbon catalysts over metal and oxide-based catalysts: the absence of the need to separate produced carbon from the catalyst [99]. Muradov also demonstrated that the catalytic activity of different carbon catalyst forms is primarily determined by their structure and surface area [102]. Other advantages of this class of catalysts include low cost and high stability during the process [103]. Carbon-based catalysts are insensitive to sulfur poisoning, which reduces methane purity requirements and facilitates natural gas pretreatment [9,103].

A number of recent review papers provide a broader perspective on carbon catalysts in CDM. For a comprehensive overview of the current state of research, including catalyst types and performance, we refer readers to the review by Hamdani et al. [44]. A more detailed discussion on how specific properties of carbon materials influence the reaction mechanism is presented by Wal and Nkiawete [55]. In addition, the effects of operating conditions on methane decomposition over carbon catalysts are examined in depth by Mirkarimi et al. [60].

Muradov et al. [104] demonstrated a correlation between the reaction rate and carbon surface area for carbon catalysts (Fig. 4B). However, the authors note that this correlation does not occur for activated carbons with a very large surface area. Suelves et al. [105] reported notable findings. They investigated CBs with different properties and concluded that the amount of carbon deposited until deactivation correlates linearly with the total pore volume of fresh catalysts (Fig. 4A).

In a series of papers, researchers reported that the presence of different defects and functional groups on the surface of the carbon catalyst was the key factor determining the rate of CDM [44,106–110]. According to Hamdani et al. [44] and Zhang et al. [109], the higher density of surface defects explains the superior catalytic properties of AC, CB, and ordered mesoporous carbons. These materials exhibit relatively high activity and the ability to tune it over a wide range.

One way to influence the surface properties of carbon catalysts is to modify their surfaces with different metal salts. For example, Wang et al. [111] added $Ca(NO_3)_2$ to activated carbon (AC), which increased the

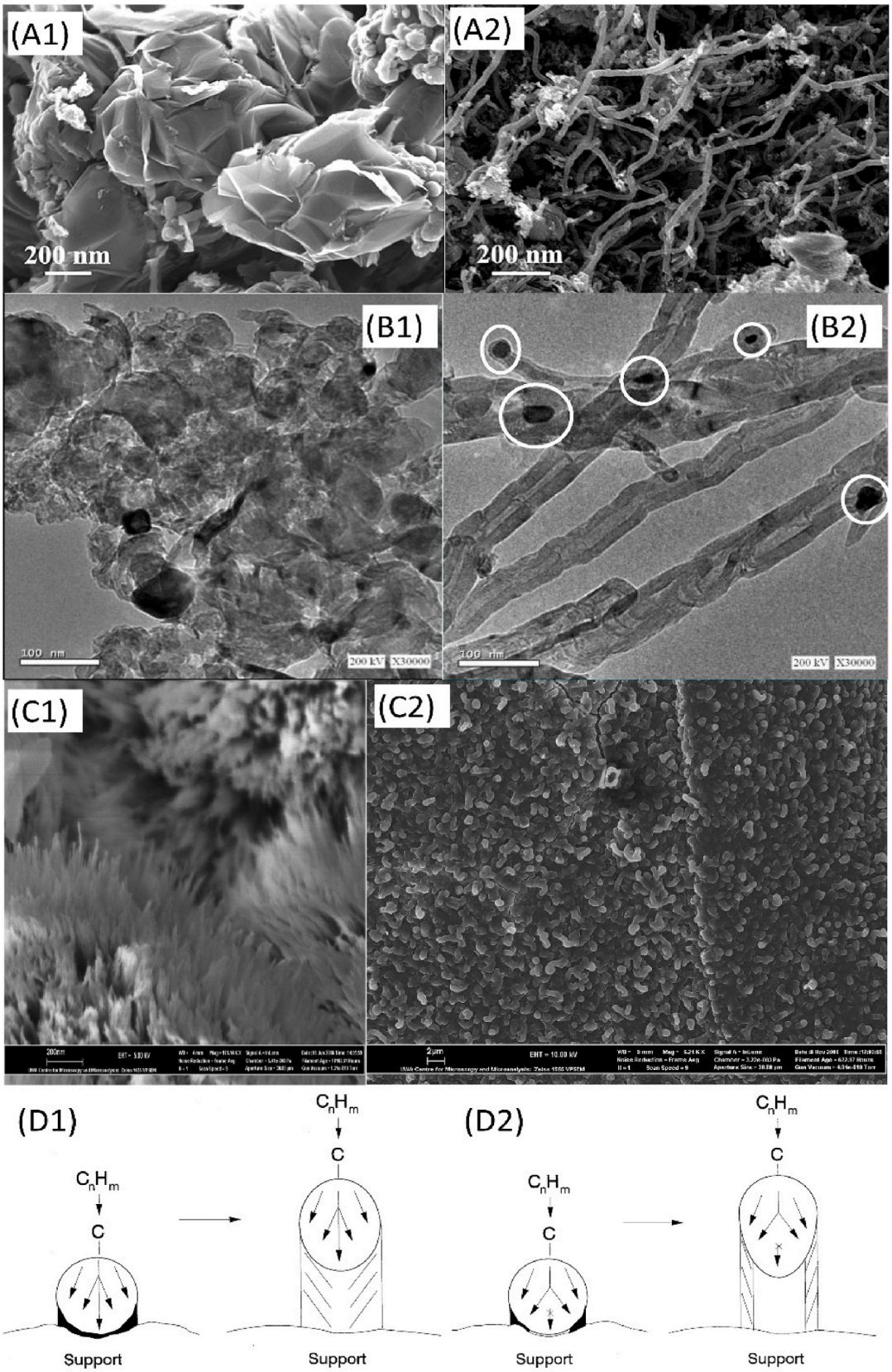

Fig. 3. FESEM of (A1) graphene sheets produced over Fe/MgO catalysts and (A2) CNT produced over Ni/MgO catalysts under the same condition [74]; TEM of (B1) CNFs and graphene films produced on Ni/Al_2O_3 and (B2) CNTs produced over Ni/CeO_2 under the same conditions [70]; carbon produced over Ni/La_2O_3 catalysts at 750°C with different methane concentrations in the gas flow: (C1) 5% and (C2) 30% [80]; schematic representations of (D1) CNF growth at low temperature and (D2) CNT growth at high temperature [81].

Table 1
Catalytic activity of various carbon-based and metal-based catalysts.

Catalyst	Synthesis	Conditions T(°C)/GHSV(L/g_{cat}/h)	Initial x_{CH_4} (%)	Time (t) (hour)	x_{CH_4} (%) at time (t)	Carbon morphology	Ref.
AC	n.d.	850/0.3	75	8	30	Graphite	[82]
AC	n.d.	900/n.d.	96	6	20	Graphene	[83]
AC (Na_2CO_3 modified)	Wet impregnation	950/0.15	100	2.5	60	Graphite	[84]
Ni/carbon	Selective gasification	850/n.d.	80	10	90	n.d.	[85]
Fe–Ni–Cu/Al_2O_3	Sol–gel	750/12	84	10	82	CNFs	[78]
Ni–Cu–Zn/MCM-22	Wet impregnation	750/30	87	60	18	CNTs	[77]
Fe–Co/MgO	Co-impregnation	700/6	45	9.5	90	MWCNTs	[86]
Ni–Fe/Al_2O_3	Sol-gel	675/24	70	10	70	CNFs and CNTs	[76]
Fe/Al_2O_3	wet impregnation	800/n.d.	79	3	84	CNFs	[87]
Fe/MgO	Sol-gel	900/9	64	3	42	MWCNTs	[74]
Fe/$CeZrO_2$	Wet impregnation	700/0.3	83	2	57	CNTs	[72]
Fe–Mo/$CeZrO_2$	Wet impregnation	700/0.3	90	2	34	CNTs	[72]
Ni/CeO_2–Al_2O_3	Co-precipitation	700/6	53	6.6	48	CNFs and CNTs	[70]
Ni@$CaTiO_3$	Direct compositing	700/18	70	4	62.2	MWCNTs	[35]
FeCo/Al_2O_3	Co-precipitation	700/17	83	10	76	Carbon nanofibers	[34]
Ni–Cu/Al_2O_3	Fusion	650/120	35	2	32	Carbon nanofibers	[33]
Ni/MgO	Evaporation induced self-Assembly	600/48	65	4	43	MWCNTs	[32]
Ni/(HZSM-5/MCM-41)	Wet impregnation	620/36	78	6	78	Graphite	[88]
NiO	Facile precipitation	800/4.5	45	6	49	Graphite and graphene	[71]
Ni–Co/CeO_2	Wet impregnation	600/36	20	2.5	16	CNTs	[89]
Fe/La_2O_3 + ZrO_2	Wet impregnation	800/4	92	4	79	Amorphous and graphite	[90]
F_2O_3	Facile precipitation	800/4.5	36	6	46	Graphite and graphene	[71]
Fe/(Al_2O_3–MgO)	Wet impregnation	800/8	87	2	87	CNTs	[91]
Fe–Co/MgO	Co-impregnation	700/6	45	9.5	86	MWCNTs	[73]
Co/Al_2O_3	Wet impregnation	700/6	81.5	7	90	MWCNTs	[92]
Co–Ni/(ZrO_2–TiO2)	Mechanical mixing	500/5	87	6	27	Graphite	[93]
Ga (liquid)	n.d.	1120/n.d.	91	n.d.	n.d.	CB	[94]
NiMo–Bi (liquid)	n.d.	800/n.d.	10	120	10	n.d.	[95]

catalyst's specific surface area from 480 m^2/g to 1119 m^2/g. This significantly increased the catalyst's activity and influenced the morphology of the produced carbon, enabling the production of carbon fibers (Fig. 4C). Similarly, Zhang et al. [112] added K_2CO_3 to carbon catalyst and observed an increase in the resulting catalyst's activity, as well as the formation of carbon fibers (Fig. 4E1). The authors attribute these effects to the transfer of oxygen from K_2CO_3 during the reaction. However, increasing the catalyst's stability comes at the cost of CO and CO_2 formation as the main reaction products (Fig. 4E2), requiring additional gas separation costs in the output stream. This also reduces the main advantage of hydrogen production from methane over other methods: the absence of CO_2 emissions.

Tzeng et al. [113] used a nickel nitrate catalyst precursor to activate carbon fiber fabrics. This modification with nickel salt significantly improved the quality of the the produced carbon. As a result, the authors succeeded in producing CNFs on the activated carbon fabrics using CDM. The obtained CNFs had a diameter between 20 and 50 nm (Fig. 4D).

Mirkarimi et al. [60] examined the impact of reaction conditions and various catalyst parameters on methane conversion. The authors showed that achieving a methane conversion of over 50% requires a temperature of over 800°C and a volume rate of pure methane of less than 1 $L/g_{cat}/h$. Additionally, applying metals such as Fe, Ni, Ca, and Pd to carbonaceous materials enhances their catalytic activity.

2.1.2. Metal-based catalysts

The first study of metal-based CDM catalysts was published by Slater in 1916 [114]. Today, it is clear that the best metal catalysts for CDM are 3d transition metals because the 3d orbitals are partially filled and can overlap with the methane orbitals [115]. This facilitates the adsorption of methane at the catalyst surface and the subsequent breaking of C–H bonds, resulting in the decomposition of methane.

The catalytic activity of transition metal catalysts for CDM is as follows: Ni, Co, Ru, Rh > Pt, Re, Ir > Pd, Cu, W, Fe, Mo [27,115]. Nickel and cobalt catalysts are active within a temperature range of 500–800°C, whereas iron-based catalysts require temperatures above 700°C [43,79]. Several recent review papers provide comprehensive insight into the design and performance of Ni- and Co-based catalysts for CDM. For Ni-based systems, Dipu [61] offers a general overview of catalyst composition, supports, synthesis methods, and reaction mechanisms. Karimi et al. [15] critically examine the promotional effects of second metals on Ni catalysts. Pham et al. [62] focus on optimizing operating parameters for Ni-based systems, while Weber et al. [63] discuss catalyst design strategies to enhance stability and productivity, particularly for Ni and Fe systems. Zeza et al. [64] provide a dedicated review of Co-based catalysts, discussing both operating conditions and catalyst design aspects for efficient methane decomposition.

However, catalytic activity is not the only parameter that determines the feasibility of using a catalyst. Stability and the ability to produce high-quality carbon are also important. For instance, depending on the size of the catalyst particles, iron-based catalysts can produce different types of CNTs: single-walled, double-walled, or thin-walled, multi-walled (Fig. 5A) [116]. The morphology of the metal particles also influences the carbon produced during the reaction. While larger particles generally increase CNT wall thickness [115] and are therefore preferable for valuable carbon products, Liang et al. [117] report that smaller particles accelerate deactivation (Fig. 5B). They explain this by stating that the proportion of uncoordinated crystallographic planes (e.g., Ni (553) or Ni(100)) is larger on small nickel particles. On these planes, the activation barriers for dissociating CH_x species are lower. Thus, the rate of carbon deposition on these particles' surfaces is higher than on larger particles', and carbon migration begins to limit the process. This, in turn, leads to the formation of encapsulated carbon species and deactivation.

Urdiana et al. [118] synthesized monometallic CDM catalysts based

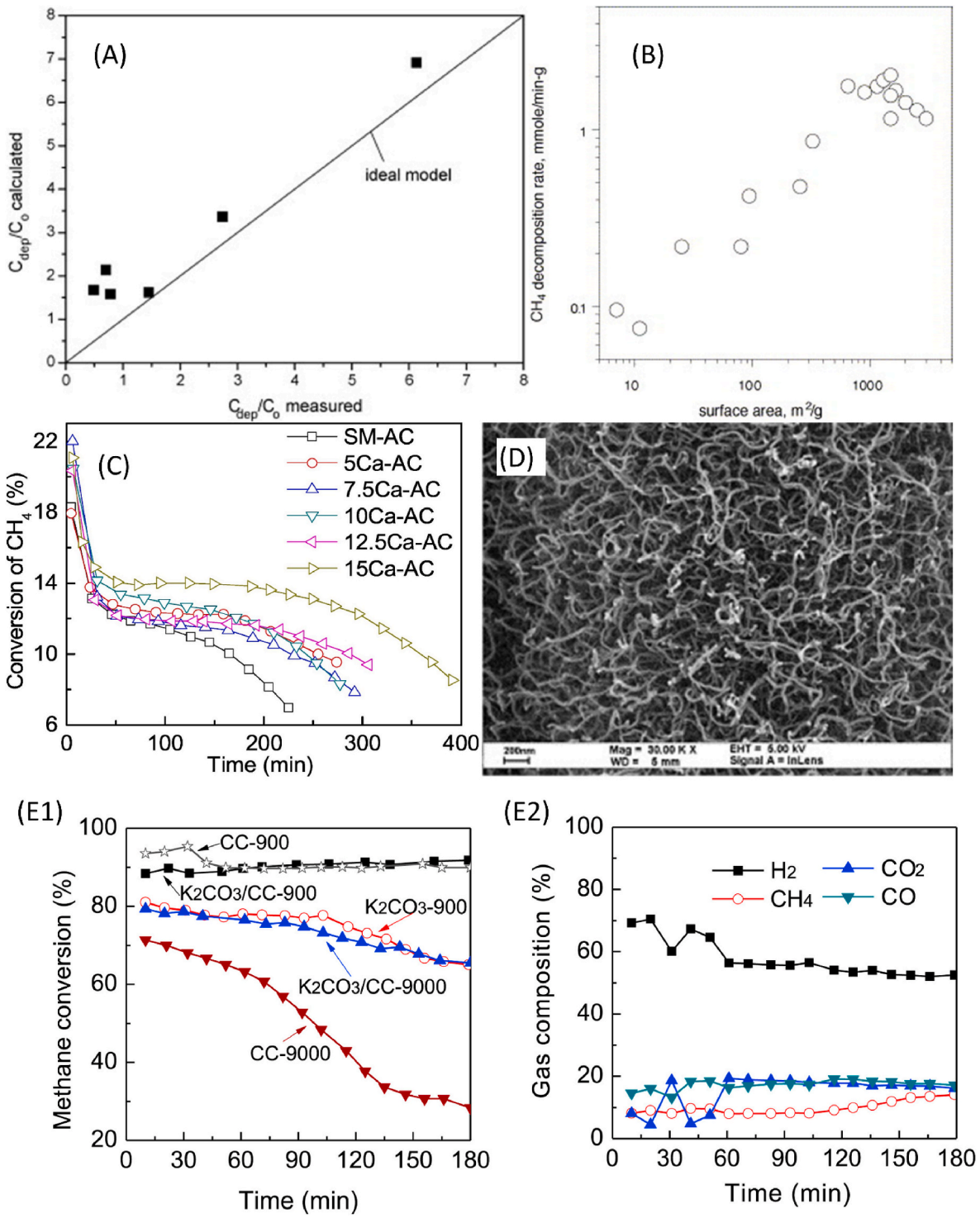

Fig. 4. (A) Calculated deposited carbon per initial catalyst mass compared to the same parameter measured when assuming that the entire pore volume is occupied by graphite [105] (B) Initial methane decomposition rate (per unit mass) as a function of carbon surface area [104] (C) Methane conversion over ACs from coal with different calcium content. (Reaction conditions: catalyst, 0.2 g; total flow rate, 50 mL/min; CH_4:N_2 1:4 (V/V); space velocity 15.000 mL/(h × g_{cat}); reaction temperature, 850°C) [111]; (D) SEM images of CNFs grown on activated carbon fiber fabric [113]; (E1)Methane conversion at 850°C and the VHSV of 900 or 9000 mL/(h × g_{CC}) using the carbon-carbon (CC) sample or the K_2CO_3/CC hybrid as the catalyst, (E2) as well as the outlet gas composition obtained over K_2CO_3 itself as the catalyst at 850°C and the VHSV of 900 mL/(h × $g_{K_2CO_3}$) corresponding to the K_2CO_3-900 sample in (E1) [112].

on nickel (Ni), copper (Cu), cobalt (Co), manganese (Mn), iron (Fe), zinc (Zn), and tungsten (W) on a mesoporous Santa Barbara Amorphous-15 (SBA-15) support. Among these catalysts, the Ni-based catalysts exhibited the greatest methane conversion at 700°C (Fig. 6). Bayat et al. [119] studied nickel catalysts in more detail. The authors prepared nickel catalysts on mesoporous, nanocrystalline gamma-alumina with different nickel loadings. They found that the activity and stability of the catalysts depended nonlinearly on the nickel loading. The catalyst with a 50 wt% nickel concentration exhibited the greatest activity and stability under CDM reaction conditions at 625 and 650°C.

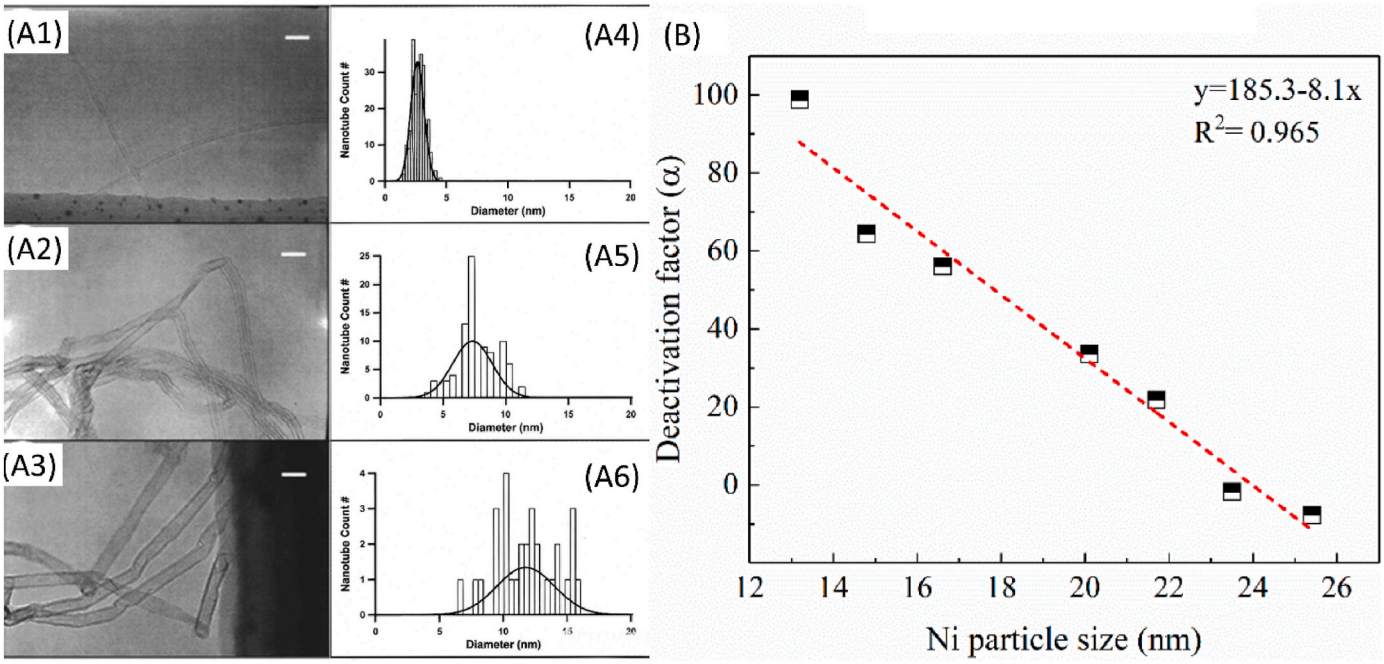

Fig. 5. TEM images of CNTs grown with iron nanoclusters, which have an average diameter of (A1) 3 nm, (A2) 9 nm and (A3) 13 nm. The scale bars are 20 nm for (A1), (A2) and (A3). The corresponding histograms of CNT diameters are plotted in (A4), (A5) and (A6), respectively. (Reprinted with permission from Ref. [116]. C. Copyright 2002 American Chemical Society); (B) Deactivation factor as a function of nickel particle size. Reaction conditions: 99.99% CH_4, total flow = 30 mL/min, catalyst loading = 0.2 g, reaction temperature: 650°C (MDPI Licence: CC BY 4.0) [117].

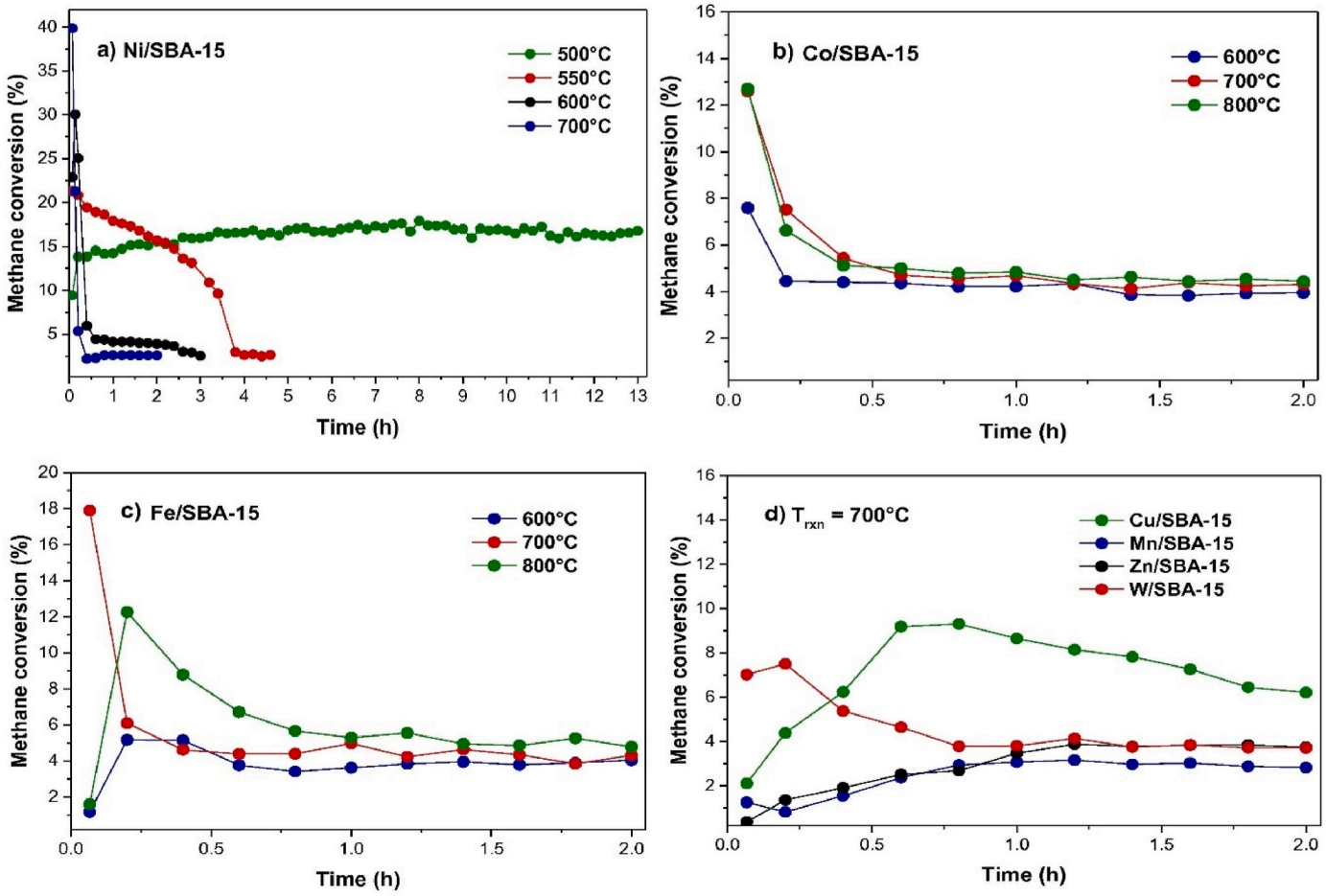

Fig. 6. Catalytic decomposition of methane using different Me/SBA-15 [118].

Although iron (Fe)-based catalysts have a higher activation energy than nickel (Ni)-based catalysts [101], they demonstrate competitive catalytic activity and greater stability at higher temperatures [25,87,120–122]. Chesnokov and Chichkan [123] showed that adding Fe to Ni-based catalysts can significantly increase stability. They compared 75% Ni–12% Cu/Al_2O_3 with 70% Ni–10% Cu–10% Fe/Al_2O_3. They demonstrated that even a small addition of Fe (10%) can substantially enhance the catalyst's stability and the quantity of carbon produced prior to deactivation (Fig. 7A). Another advantage of Fe-based catalysts is their relatively low cost [43,115,124].

For example, Abdel-Fattah et al. [125] investigated unsupported Fe–Al and Co–Al catalysts for CDM at 800°C and a GHSV of 2.4 L/g_{cat}/h. The Co–Al sample contained $CoAl_2O_4$ and Co_3O_4. The Fe–Al catalyst consisted of Fe_2O_3 (65.4%) and $FeAl_2O_4$ (34.5%). This catalyst exhibited stable 95% methane conversion over 5 h. TEM images of the spent catalysts revealed different forms of deposited carbon. Filamentous carbon deposited on the spent Co–Al catalyst took the form of carbon nano-onions (CNOs) (Fig. 7B1-B2) and MWCNTs, whereas bamboo-like CNTs were the main form of deposited carbon on the spent Fe–Al catalyst (Fig. 7B3-4). The shape of the deposited carbon explains the Fe–Al catalyst's higher activity and stability in CDM compared to the Co–Al catalyst.

Qian et al. [126] investigated Fe–Mg–O catalysts for CDM. The researchers prepared a series of catalysts with Fe/Mg molar ratios ranging from 3:1 to 1:3. For Fe:Mg > 1, the catalysts consist of a mixture of Fe_2O_3 and $MgFe_2O_4$ spinels. These spinels must undergo an additional phase transition to form the CDM-active structure with the metal iron (Fe). For Fe:Mg < 1, longer incubation times were observed (Fig. 7C1-2). The samples contain mixtures of MgO and $MgFe_2O_4$ spinel in their fully calcined states. Consequently, the catalysts with Fe:Mg > 1 did not become active for C–H cleavage. The catalyst with a molar ratio of 1:1 showed the best performance (48% methane conversion and a carbon yield of 8.6 g_C/g_{Fe}) (Fig. 7C3-4). The authors explain that a higher Fe:Mg ratio results in larger metal-Fe particles with significant agglomeration. In contrast, a smaller Fe:Mg ratio results in insufficient metal-Fe sites for methane activation. The generated carbon structure consisted of CNTs, CNOs, CNFs, and graphene sheets, and was the same for all samples.

A number of studies [73,92,127–129] have investigated Co-based catalysts and shown their high stability at high temperatures. However, the wider use of cobalt is limited due to its toxicity. Additionally, proper selection of support can significantly improve the catalytic properties and durability of Co catalysts [92,130,131].

Awadallah et al. [128] investigated cobalt (Co) and nickel (Ni) on aluminosilicate hollow sphere catalysts for CDM. The support material reduced the aggregation of the active metal particles. Additionally, this support allows greater dispersion of the active metal phase. As the authors point out, the Co/Si–Al catalyst exhibited higher activity over a longer reaction time than the Ni-based catalyst (Fig. 7D). They explain this difference by the formation of Ni_2SiO_4 in the Ni/Si–Al sample, which renders a significant portion of the Ni inactive in the reaction. Conversely, the large number and higher dispersion of non-interacting Co_3O_4 on the catalyst surface improved the catalytic efficiency of the Co/Si–Al catalyst. According to the TEM and Raman spectroscopic data, MWCNTs formed on both catalysts.

Mesfer et al. [131] investigated TiO_2–Al_2O_3-supported Co-based catalysts with a cobalt loading ranging from 43% to 74%. They reported that the cobalt metal exhibited high activity and a long catalyst lifetime, probably due to high metal dispersion. They also found that cobalt loading significantly affected the catalysts' activity and stability. Activity and stability were found to be directly proportional to cobalt loading. The highest metal loading provides the greatest methane conversion and catalyst stability (Fig. 7E).

However, recent studies [25,76,78,132,133] have found that monometallic catalysts, consisting of only one metal, are usually inferior to polymetallic catalysts consisting of an alloy of several active elements. For instance, adding iron to nickel catalysts increases the carbon diffusion rate, reducing deactivation and enhancing stability. It is also known that adding copper improves the performance of nickel catalysts [33,77]. Although copper itself is not involved in the reaction, it attracts formed carbon due to its high affinity for carbon, thereby preventing encapsulation of the nickel active sites [76,78]. Adding cobalt to an iron catalyst inhibits carbide formation and increases the catalyst's lifetime [133]. The role of molybdenum in polymetallic catalysts is particularly noteworthy.

Awadallah et al. [134–136] and Liang et al. [137] studied the effects of adding molybdenum (Mo) to nickel (Ni) or cobalt (Co) catalysts. The Co–Mo/MgO catalyst exhibited higher catalytic stability over a longer reaction time than similar catalysts without Mo doping (Fig. 8A1). Additionally, TGA revealed that the Co–Mo/MgO exhibited ерy higheые CNT yield during CDM (Fig. 8A2) [136]. Liang et al. showed that the NiMgAlMo catalyst had higher catalytic activity than the NiMgAl catalyst derived from untreated NiMgAl layered double hydrotalcite under all selected reaction conditions. Incorporating Mo into Co/MgO increases the catalytic stability for CDM over long reaction times. The NiMgAlMo catalyst achieved an excellent hydrogen formation rate of 60.4 mmol/g_{Ni} min at 700°C (Fig. 8B). After ten consecutive CDM/air/hydrogen reaction and regeneration cycles, the NiMgAlMo catalyst demonstrated stability with only a slight decrease in the H_2 formation rate.

Rastegarpanah et al. [138] doped the Ni/MgO catalyst with metals from Group VIB. They demonstrated that chromium (Cr) doping significantly increased the catalytic activity and stability of the Ni/MgO catalyst system (Fig. 8C). Additionally, the carbon generated over Cr-doped catalysts exhibited higher purity, and a higher degree of crystallinity.

Wang et al. [139] added various metals (Cu, Mn, Pd, Co, Zn, Fe, and Mg) to Ni/Al_2O_3. In all cases except with zinc, the stability and activity of the catalytic system improved (Fig. 8D). Changing the metal composition can significantly impact the interaction between the active metal and the support, thereby improving the activity and stability of the catalytic system. The authors attribute this to an increase in surface area, a higher concentration of oxygen species, and improved reducibility.

Using a supported catalyst can improve dispersion, prevent the aggregation of active catalyst particles, and increase the catalyst's specific surface area and structure [115]. For CDM, metal oxides are typically used as supports. Examples include: MgO [32,138], Al_2O_3 [32,139], SiO_2 [32,140], CeO_2 [141], TiO_2 [32,142], La_2O_3 [143], ZrO_2 [32,144], Y_2O_3 [145].

The concentration of active sites is one of the most important indicators influencing the properties of the heterogeneous catalytic system. Regarding CDM metal catalysts, Sikander et al. [146] discussed this topic in detail. The authors synthesized nickel catalysts based on hydrotalcite ($Mg_6Al_2(OH)_{16}CO_3{\cdot}4H_2O$). A catalyst with a nickel concentration of 40 wt% showed the best performance (methane conversion of more than 80% during 7 h of gas flow at 650°C) (Fig. 8E). As the loading concentration increases, the size of the nickel particles increases, as does their structural change. Therefore, the sintering of the active sites leads to a deterioration in the overall rate of methane conversion.

Calgaro et al. [147] came to similar conclusions with Co/Al_2O_3 catalysts containing 50–100 wt% of cobalt. They achieved better catalyst performance with 50 wt% cobalt. Further increasing the Co content leads to larger crystallites, decreased methane conversion, and faster deactivation.

Although metal-based catalysts are less durable and cost more than carbon-based catalysts, they currently exhibit higher methane conversion [25]. In general, using supports offers great potential for altering the activity and stability of the catalyst. Polymetallic supported catalysts are emerging as a key pathway toward improving the performance and long-term stability of CDM processes.

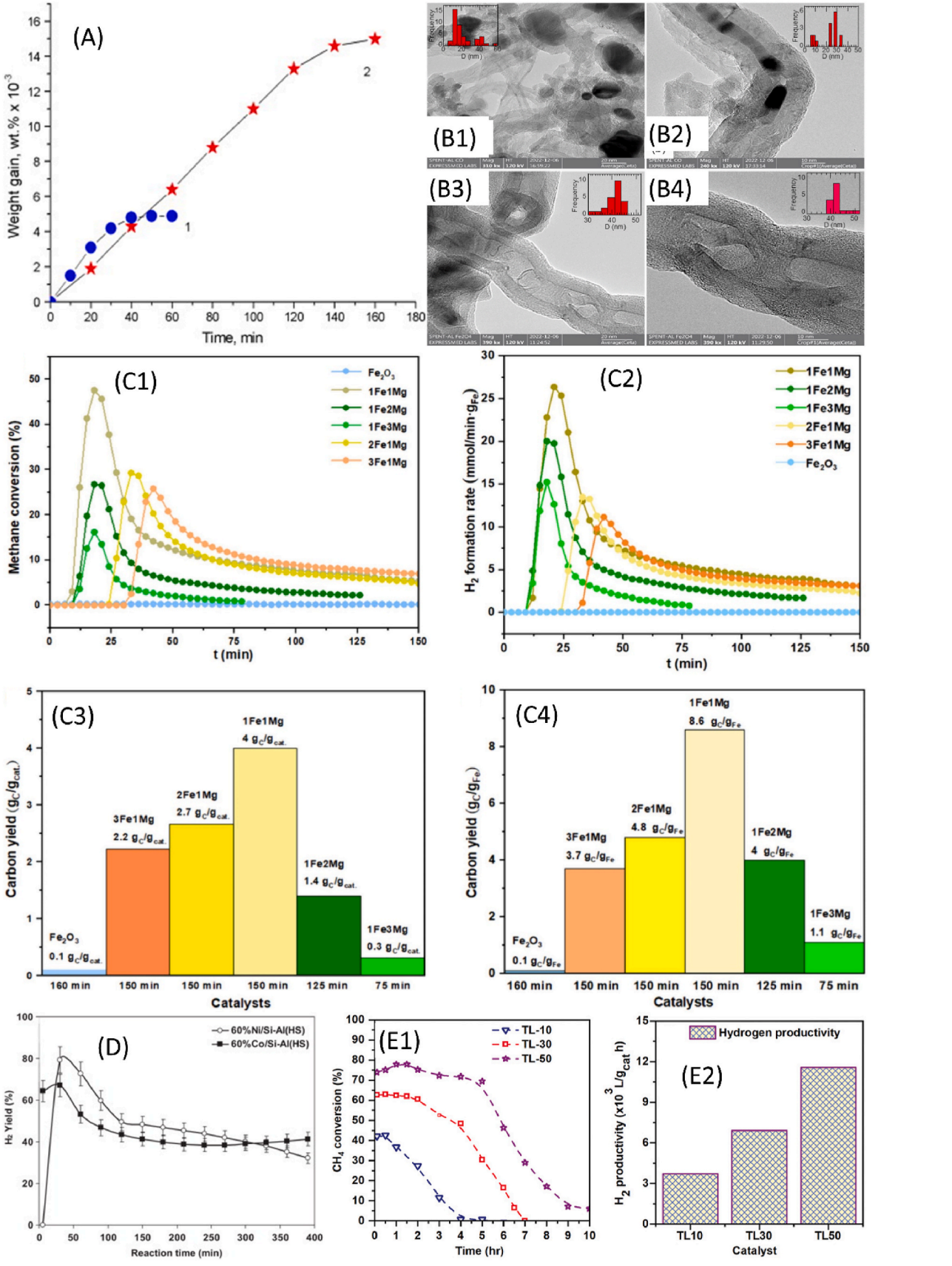

(caption on next page)

Fig. 7. (A) Kinetic curves of carbon deposition over 75%Ni–12%Cu/Al_2O_3 (1 - blue circles) and 70%Ni–10%Cu–10%Fe/Al_2O_3 (2 - red stars) catalysts from methane at 700°C [123]; TEM images of spent (B1,2) Co–Al and (B3,4) Fe–Al catalysts. The inset shows the histogram of the diameter distribution of the carbon nanostructure [125]; (C1) Profile of the methane conversion as a function of throughput time on the different fresh catalysts. Reaction conditions: 50 mg catalyst, 850°C (heating rate = 10°C/min), CH_4 flow rate of 15 mL/min; (C2) Profile of H_2 formation rate as a function of time in stream over the different fresh catalysts. Reaction conditions: 50 mg catalyst, 850°C (heating rate = 10°C/min), CH_4 flow rate of 15 mL/min; Carbon yield, reaction condition: 50 mg catalyst, 850°C (heating rate = 10°C/min), CH_4 flow rate of 15 mL/min (C3) normalized to the mass of the catalyst or (C4) normalized to the mass of iron [126]. (D) hydrogen yield through CDM vs. reaction time at 700°C using 60%Ni/Si–Al and 60%Co/Si–Al catalysts [128]; Results of (E1) TOS study and (E2) hydrogen productivity (reaction at 600°C, 1 bar feed gas CH_4: Ar = 1:1 and GHSV = 1.8 × 104 mL g^{-1} h^{-1}) [131].

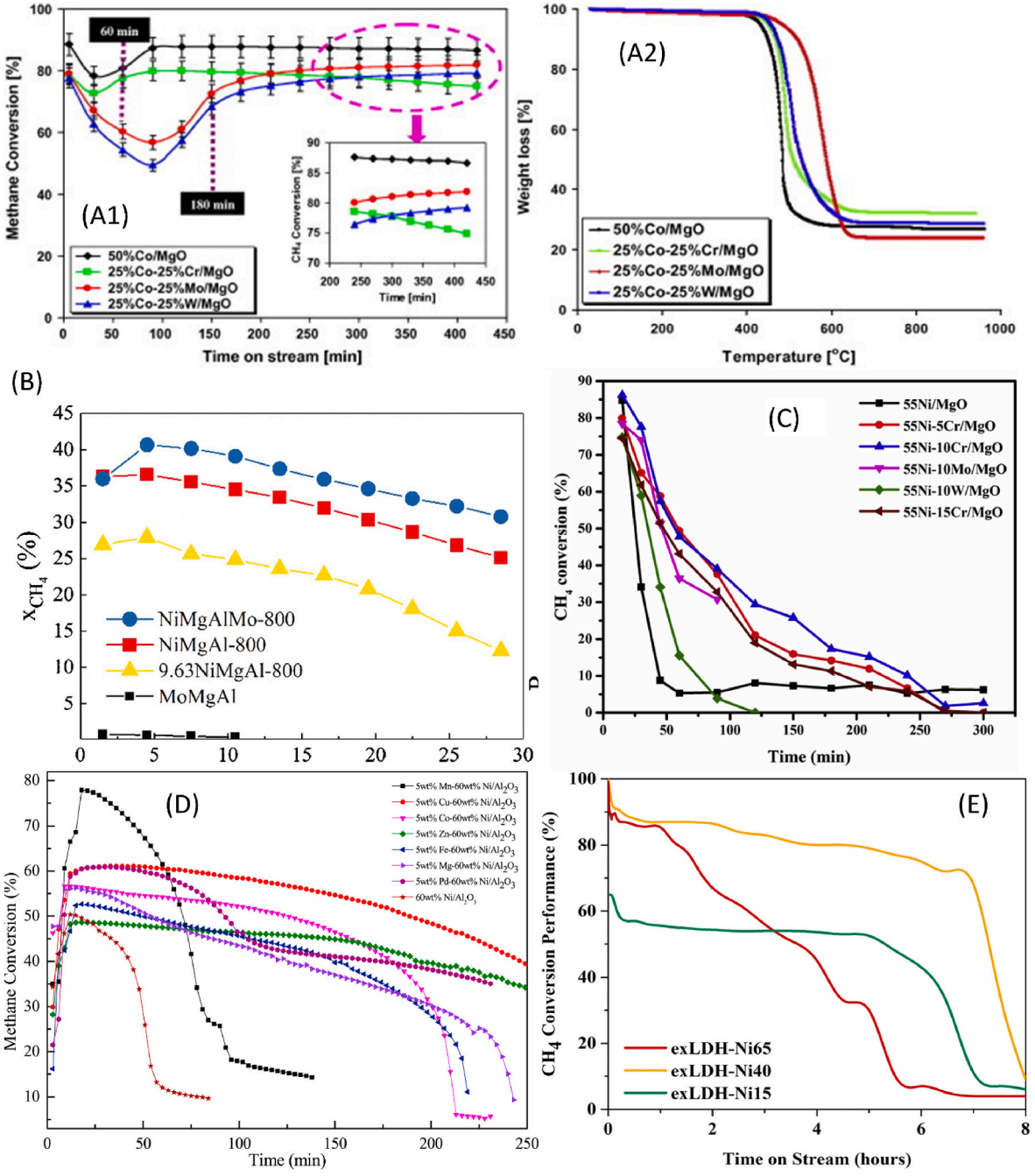

Fig. 8. (A1) Methane conversion as a function of time-on-stream over mono- and bimetallic cobalt-based catalysts [136] (A2) TGA analysis of CNTs produced over used catalysts 50%Co, 25%Co–25%Cr, 25%Co–25%Mo and 25%Co–25%W/MgO [136]. (B) Methane conversion versus the reaction time over the NiMgAl-800, 9.63NiMgAl-800 and NiMgAlMo-800 catalysts. Reaction conditions: 99.99% CH4, total flow = 30 mL/min, catalyst loading = 0.2 g, reaction temperature: 650°C [137]. (C) Stability tests of catalysts with various metal doping at 675°C. Reaction conditions: CH_4:N_2 volumetric ratio = 15:85, GHSV = 48,000 mL/(g × h) [138] (D) Effect of different 5 wt% M-60 wt% Ni/Al_2O_3 catalysts on methane conversion [139] (F) The methane conversion performance of hydrotalcite-based catalyst with various Ni loading tested at 650°C [146].

2.1.3. Molten catalysts

The limitations of solid-based catalysts, particularly their deactivation by coke encapsulation and sintering, have prompted researchers to seek alternatives, such as molten catalysts for methane pyrolysis. These catalysts can generally be divided into two categories: molten metals and molten salts. In the context of catalytic methane decomposition, molten catalysts have become a particularly active research topic due to their resistance to carbon-induced deactivation. For those interested in a more comprehensive overview of the current state of molten catalyst development for CDM, we recommend several recent review articles on this subject [45,46,65,66].

Molten catalysts are less susceptible to deactivation by carbon deposits because solid carbon particles can more easily be removed from the liquid catalytic phase. For example, this can be done using a bubble column reactor. In practice, highly catalytically active metals, such as nickel (Ni), are diluted with less active metals to lower the melting point. Bi and Sn, for example, are often used as "solvents" [148,149].

The CDM reaction was also tested with Mg [150] and Te [151] as molten metal catalysts. Although Mg and Te cannot be compared directly due to differences in reactor design and operating conditions, both catalysts demonstrated quantitative methane conversion (Fig. 9A). Although molten metal catalysts are protected from deactivation by carbon deposits, this does not mean that this approach is flawless. The main problems with molten catalysts are their evaporation and the resulting metal contamination of the produced carbon. Wang et al. [150] believe this problem can be solved with uniform noncatalytic molten metal systems, in which the molten metal serves only as a heat transfer medium for noncatalytic methane decomposition. Geiβler et al. [152] obtained promising results in a 1 m bubble column with molten tin, reaching 78% methane conversion at 1175°C (Fig. 9B). Upham et al. [148] performed a systematic screening of Ni, Pt, and Pd in molten Bi, In, Ga, Sn, Pb, and Ag and Au (21 variants in total) to determine the catalytic effect of combinations on methane pyrolysis. A Bi–Ni alloy with 27 mol% Ni proved to be the most efficient at 1000°C. Building on this work, Palmer et al. [153] investigated the Cu–Bi alloy. They found that molten Cu–Bi is an active catalyst, even though pure molten Bi and Cu are not. Based on theoretical calculations, authors concluded that interaction with copper alters the electron density of bismuth, imparting catalytic properties to electron-deficient bismuth and promoting methane dissociation.

Another noteworthy aspect is the use of molten salts to prevent the catalyst from deactivating. Although other processes, such as cellulose

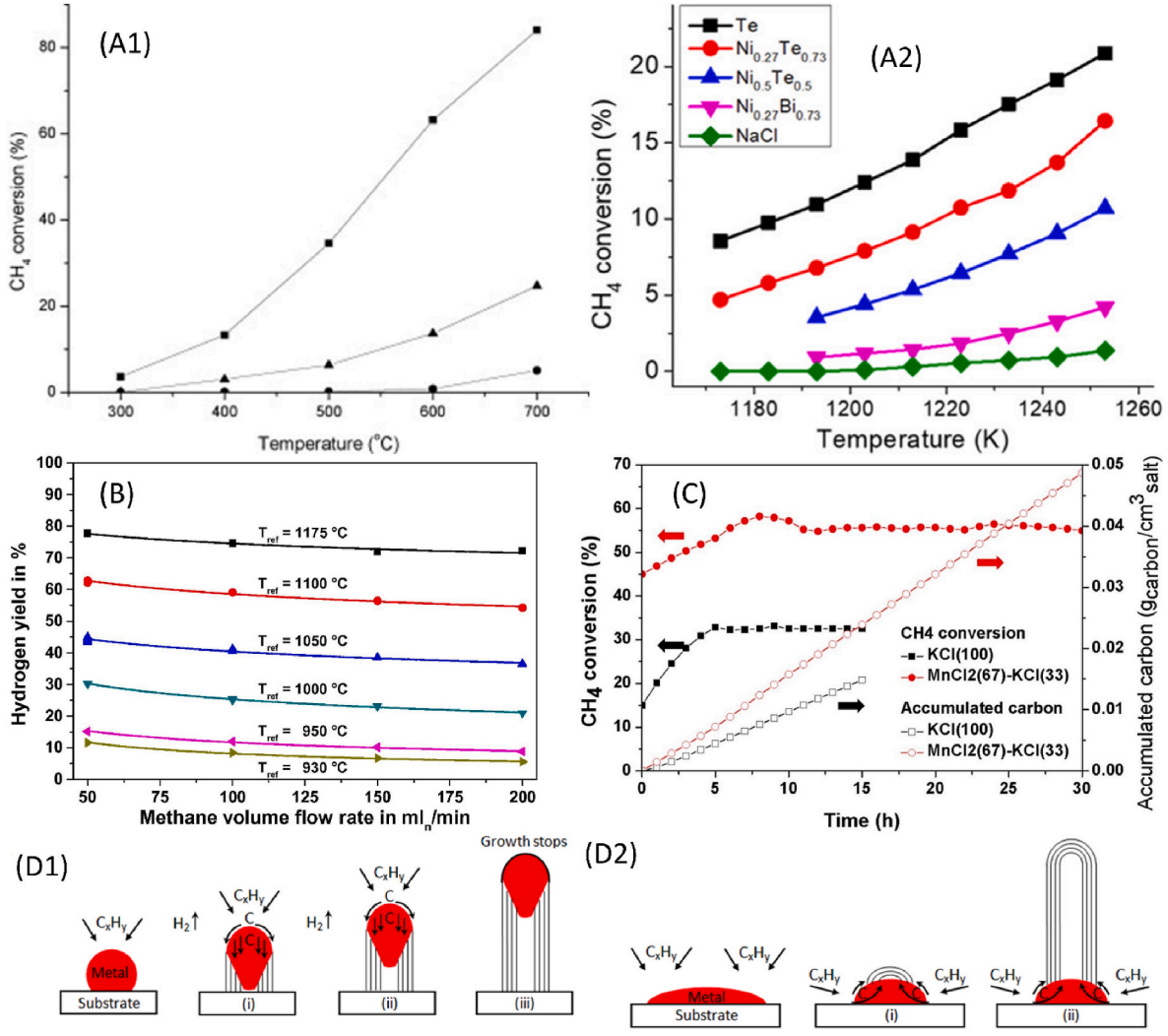

Fig. 9. (A1) Methane conversion at different temperatures. (●) Without catalyst, (▲) over molten Mg, and (■) the equilibrium conversion of methane according to the thermodynamic calculation [150] (A2) CH_4 conversions in 7-cm bubble column reactors over different melts. The partial pressure of CH_4 was 0.7 atm, the bubble diameter ~5 mm, and the residence time about 0.5 s (Reprinted with permission from Ref. [151]. Copyright 2020 American Chemical Society) (B) Hydrogen yield over liquid tin as a function of methane volume flow rate at different reference temperatures with pure methane as feed gas [152] (C) CH_4 conversion over 30 h of continuous operation for the 12.5 cm bubble columns of molten $MnCl_2$(67)-KCl(33) and KCl(100) at 1050°C: reactant gas = 5 sccm (100 mol% CH_4), sweep gas = 50 sccm (100 mol% Ar) [156]; (D1) Tip and (D2) base carbon growth mechanisms [159].

pyrolysis and methane reforming, sometimes use molten salts with solid catalysts, CDM reactions typically use liquid salts with molten metal catalysts. The promoting effect of the molten salt may be due to its improved wettability with the Fe–Ni alloy, which can prevent deactivation of the catalyst due to carbon encapsulation [154]. Typically, the molten salt forms an additional liquid layer in the bubble column, above the liquid metal. This ensures that the resulting carbon does not touch the metal's surface, but rather floats on the molten salt's surface. Some molten salts have catalytic properties, and their catalytic mechanism is generally similar to that of solid catalysts. CDM catalysis in molten salts mainly uses alkali metal halides [155–158]. Their catalytic activity is generally similar to that of CDM over metal catalysts [155]. Hydrogen atoms consistently split off from the methane molecule to form hydrogen and carbon at the gas-liquid phase boundary.

Alkali metal halides are typically added to the halides of other metals, such as $MnCl_2$ and $FeCl_3$. Various authors explain this phenomenon through the formation of complexes with lower activation energy [156,158]. This can significantly increase the activity and hydrogen selectivity of molten salts. For example, Kang et al. [156] reported that the $MnCl_2$–KCl (67:33) system exhibited 99 %H_2 selectivity at 1050°C, whereas pure KCl demonstrated only 90% selectivity under the same conditions. Meanwhile, the molten $MnCl_2$–KCl system provided stable 50% methane conversion for 30 h (Fig. 9C). Pure KCl exhibits relatively high selectivity for hydrocarbon intermediates, such as ethylene, acetylene, and aromatics [156,158]. However, a possible explanation for this phenomenon lies in the formation of insoluble reduced metal particle aggregates. Attempts have been made to use halides of other metals that can form Lewis acids, such as nickel (Ni), cobalt (Co), and copper (Cu), but they are too rapidly reduced to metals [158].

2.2. Long-term operational issues

One of the main obstacles to commercializing CDM is catalyst deactivation due to carbon deposits blocking the catalyst's active sites. Therefore, many authors consider regenerating spent catalysts one of the main tasks for commercializing CDM [9,25,27,61,62,109,160–162]. However, it is often overlooked that most regeneration processes destroy the valuable carbon products, which undermines CDM commercialization efforts. Thus, technologies that capture valuable carbon products are also important [41,66,109,162].

2.2.1. Catalysts deactivation and regeneration

The main problem with commercializing CDM is the deactivation of solid catalysts due to carbon covering their active sites. Tong et al. [47] and Välimäki et al. [48] accurately reviewed the literature on the mechanisms of deactivation and carbon formation. These reviews both emphasize the importance of the growth mechanisms of CNTs: tip growth and base growth. One or the other is active depending on the strength of the interaction between the catalyst metal and the support (Fig. 9D). Takenaka et al. [163,164] investigated Fe- and Co-based catalysts and demonstrated that the tip-growth mechanism provides higher methane conversion and catalyst stability. However, the tip-growth mechanism renders the catalysts incapable of regeneration. Torres et al. [165] investigated different types of doping for Ni catalysts and found that doping with copper can significantly decrease catalyst deactivation. Avdeeva et al. [166] compared supported and non-supported Ni catalysts and found that the support prevents metal particles from being encapsulated by carbon and becoming inactive. Opinions about the influence of catalyst size are varied. Ashik and Doud [167] synthesized SiO_2 supported Ni, Fe, and Co and investigated their catalytic properties for CDM. The authors concluded that larger particles have a smaller surface area, causing the samples to deactivate rapidly. However, Liang et al. [117] and Christensen et al. [168] found that small particles deactivate faster than large ones. Liang et al. [117] explained this phenomenon by stating that "carbon nanotubes, which maintain catalyst activity, are more likely to form on large nickel particles, while encapsulated carbon species, which lead to deactivation, are more likely to deposit on small particles." Christensen et al. [168] explain this phenomenon by the higher saturation concentration of carbon in smaller nickel crystals.

There are three main methods for the regeneration of solid metal catalysts after deactivation caused by carbon deposition [25], all of which are based on oxidizing of the generated carbon into its oxides such as CO and CO_2. These methods include carbon combustion in atmospheric oxygen [169–173] (eq. (5)), steam regeneration [172,174] (eq. (6)) and carbon dioxide regeneration [82,175,176] (eq. (7)).

$$C + O_2 \leftrightarrow CO_2 \tag{5}$$

$$C + H_2O \leftrightarrow CO + H_2 \tag{6}$$

$$C + CO_2 \leftrightarrow 2CO \tag{7}$$

One of the main problems in catalyst regeneration is the sintering of catalyst particles during the process [177]. Among the presented regeneration methods, steam regeneration has the advantage of avoiding sintering if the reaction temperature is properly controlled. This mitigates a decrease in the catalyst's specific surface area and activity in subsequent operating cycles [170].

However, as pointed out in references [9,27,109], a rather novel approach to solving the problem of regenerating solid, metal-based catalysts was proposed. The authors tested the Fe/CaO–$Ca_{12}Al_{14}O_{33}$ catalyst and its regeneration efficiency in cyclic CDM and regeneration experiments. They separated the catalyst and the carbon deposit using vibratory separation. Approximately 10% of the carbon deposit consisted of high-quality CNTs. The remaining carbon was removed via steam gasification. The resulting carbon dioxide was captured by CaO, forming $CaCO_3$. Calcination then produced CaO and pure CO_2. After eight cycles, the catalyst's methane conversion decreased from 90% to 80%.

Chu et al. [178] proposed a innovative approach to solving the problem of regenerating solid, metal-based catalysts. The authors tested the efficiency of regenerating the Fe/CaO–$Ca_{12}Al_{14}O_{33}$ catalyst in CDM/regeneration cycles. They separated the catalyst and the carbon deposit using vibratory separation. Approximately 10% of the carbon deposit consisted of high-quality CNTs. The remaining carbon was removed via steam gasification. The resulting carbon dioxide was captured by CaO to form $CaCO_3$. Calcination then produced CaO and pure CO_2. After eight cycles, the catalyst's methane conversion decreased from 90% to 80%.

2.2.2. Produced carbon separation

For carbon-based catalysts, separating the carbon product from the catalyst is unnecessary [179]. Using molten metal catalysts solves the problem of separating generated carbon from the catalyst because the carbon can easily be collected from the liquid surface due to its lower density. However, the carbon usually requires additional purification to be utilized [180]. Therefore, the main problems in separating carbon products from catalysts are specifically related to solid metal-based catalysts.

Vibrational separation is the most widely used method for separating the catalyst from the produced carbon. Hatanaka and Yoda [181] used mechanical regeneration by shear stress to remove carbon from the $FeTiO_3$ catalyst in situ. In this device, a vortex flow was generated by gas fed along the inner surface of a tube at the upper and lower ends of the regeneration device (see Fig. 10A). The vortex flow caused the catalyst particles with carbon deposits on their surfaces to rotate in the tube. The particles were subjected to shear stresses due to collisions among the particles and with the wall. This, in turn, caused the carbon deposits to be removed from the catalyst surface. The separated carbon was collected by filters at the reactor's outlet. The carbon mass content on the filters was 84%. Sixteen percent of the carbon remained in the

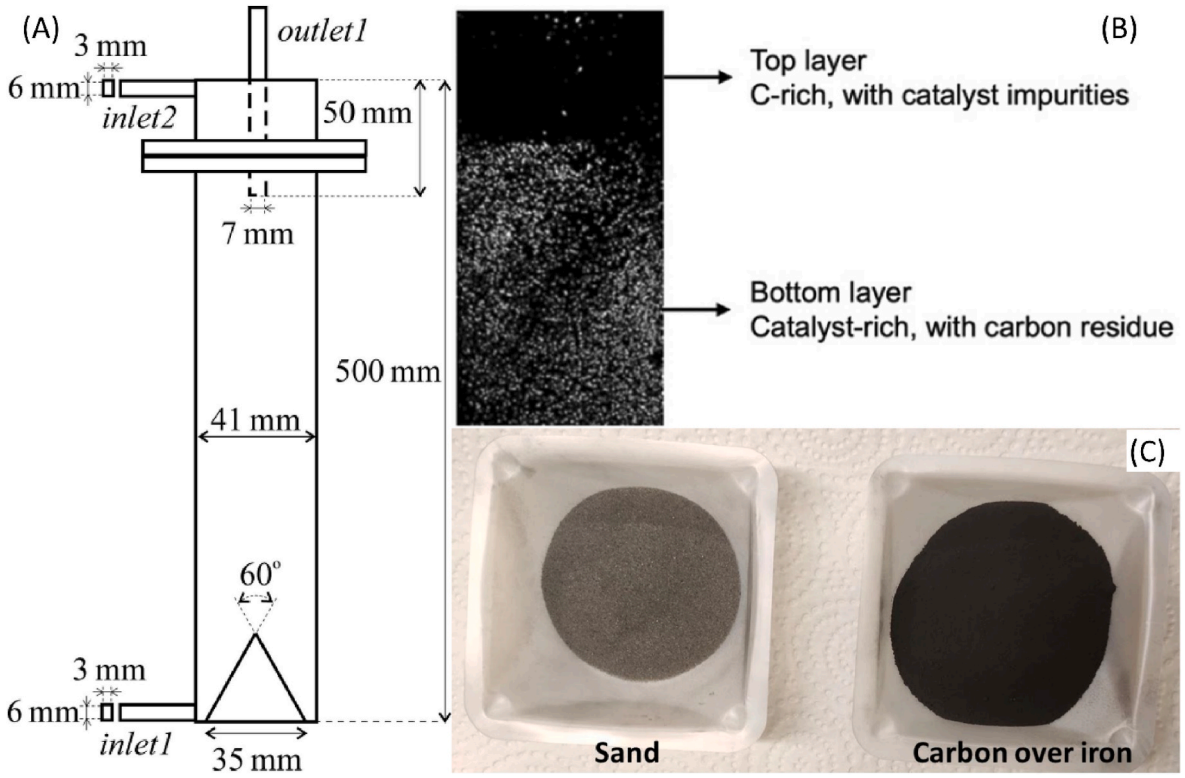

Fig. 10. (A) Device for the regenerating of catalyst particles [181] (B) Photographic representation of vibrational separation [182] (C) Solids removed from the reactor after magnetic separation (S. Pathak and E. McFarland. License: CC BY 4.0) [184].

sample. Over the course of nine operating cycles, each lasting 60 min, the methane conversion rate decreased from 96% to 81%.

Yang et al. [182] demonstrated the applicability of a vibrating fluidized bed with a carbon catalyst (Fig. 10B). The inner diameter of the bed was 4 or 8 cm. The 12–15 cm bed consisted of spent catalyst and carbon products. The oscillation frequency could be increased from 15 to 50 Hz, with an amplitude ranging from 0.03 to 0.06 cm. The deposited upper CNT layer could be removed in batches with a suction probe. The spent catalyst was removed from the bottom of the vibrating bed. The deposited CNT layer was also removed in batches with a suction probe. The spent catalyst was removed from the bottom of the vibrating bed. A simulation experiment was carried out to fluidize a mixture of CNTs and catalyst. The results showed that the upper carbon layer of the fluidized bed contained 99.4% CNTs due to fluidization, while the lower catalyst layer contained only 0.35% CNTs. However, in the case of a true mixture of reaction products and catalyst, the upper layer consists of only 57% carbon, while the catalytic mixture accounts for the remaining 43%. The authors concluded that vibrational separation was insufficient due to the strong metal-CNT bonds. To purify the CNTs, the authors subjected them to additional filtration through a dense medium, followed by leaching with HCl and KOH to remove metal impurities. The results demonstrated the feasibility of the multi-stage approach, which a preliminary economic analysis confirmed.

It is also worth noting that many metallic catalysts, such as Ni, Co, and Fe_3O_4, are ferromagnets that can be used to separate the catalyst from carbon deposits. For example, Keller and Sharma successfully used magnetic separation to separate catalytic magnetite particles from ZrO_2 supports [183]. Pathak and McFarland [184] later used a similar technique to separate magnetic iron particles from the inert diluent used in the fluidized bed reactor (Fig. 10C). However, due to the strong interaction between metals and CNTs, this approach can hardly be used without combining it with other methods to separate the metal catalyst from the CNTs.

Wang et al. [185] proposed another way to separate high-value CNTs from the metal catalyst. Building on previous work on purifying CNTs from impurities through controlled oxidation in nitric acid [186–188], the authors placed the spent catalyst containing the produced CNTs under reflux for 24 h. The metal catalysts were oxidized, and the resulting CNTs were analyzed using XRD, Raman spectroscopy, SEM-EDX, TEM, and TGA. The results showed that the catalyst had been completely removed from the CNTs, which retained their crystallinity. The resulting CNTs were pure and highly stable.

2.3. *Reactors for catalytic decomposition of methane*

There are several types of reactors for CDM. These include reactors with solid catalysts, reactors with liquid catalysts, and reactors with a plasma catalyst. The most important types are shown in Fig. 11. Operating conditions significantly influence the results of the process, including methane conversion, process stability, and the type of carbon produced. The following two overviews contain detailed descriptions of reactor systems that can be used in CDM. Sanyal et al. [49] emphasize the importance of the operating conditions of the reactor. Raza et al. [50] provide a broader overview of different reactor types, covering not only the basic reactors but also more specific types.

2.3.1. *Fixed bed reactor*

In the fixed-bed system, the catalyst is placed in a stationary bed inside the tubular reactor, while the gas flows through it (see Fig. 11A2). The reactor is then heated to the desired temperature. For the CDM reaction, the reactor can be equipped with a filter system or separator to capture solid carbon particles in the outlet flow.

The fixed bed system can be used with all types of solid catalysts: carbon, metals, and metal supports [191–197]. The fixed-bed (FBR) was the first chronologically used CDM reactor. Due to its simplicity, this type of reactor is the most commonly used for CDM [78,120]. However, the fixed-bed reactor has a major disadvantage for the CDM reaction: it can clog from the carbon produced during the reaction. Nevertheless,

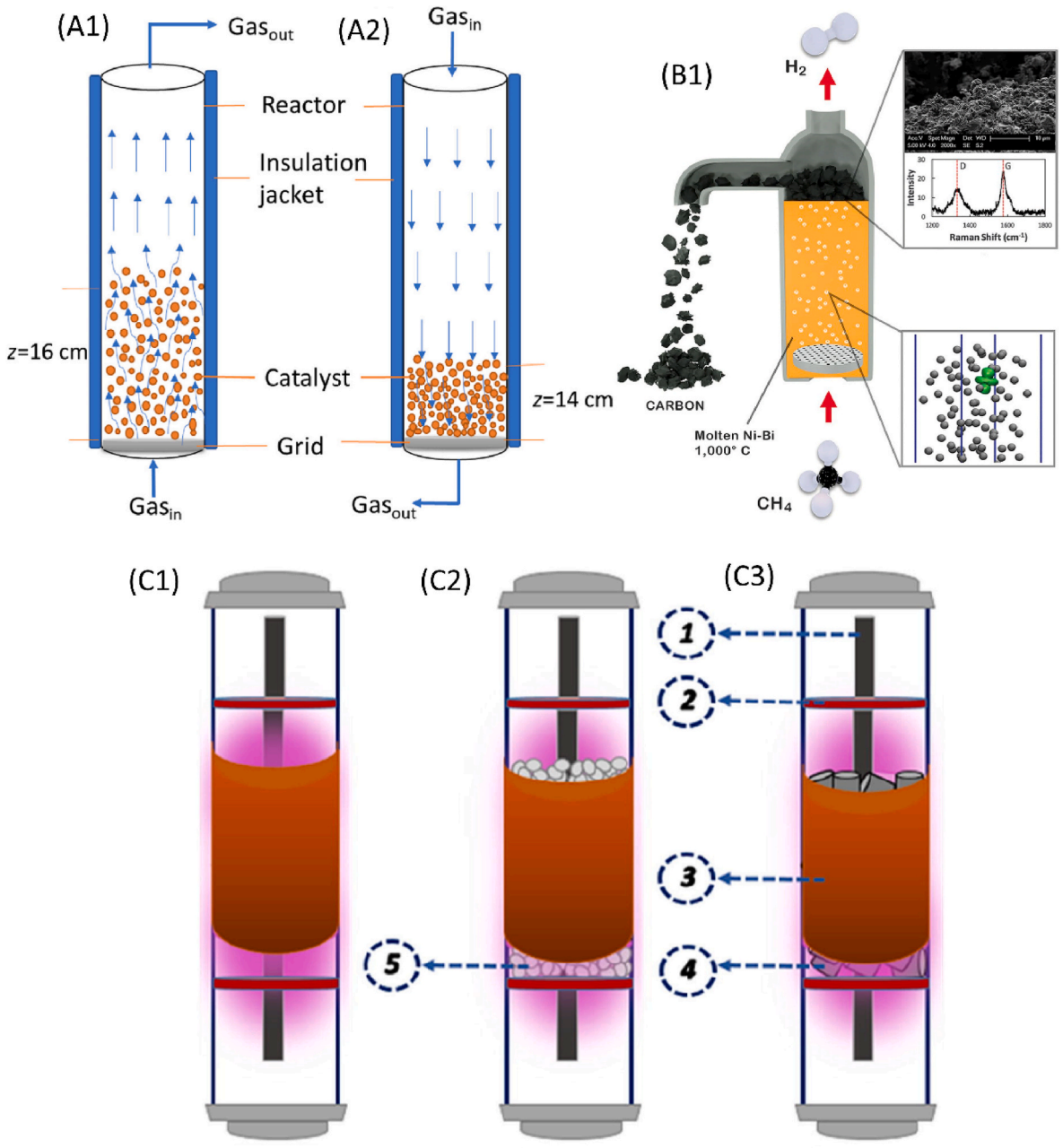

Fig. 11. Various reactors suitable for H_2 production by CDM; (A1) fluidized bed reactor with gas inlet from below; (A2) fixed bed reactor with gas inlet from the top (T.N.Eran et al. Licence: CC BY 4.0) [189]; (B11) reactor for the conversion of CH_4 to H_2 and carbon in a molten metal bubble column with continuous carbon removal [148]; three types of plasma system: (C1) pure plasma, (C2) packed plasma, (C3) catalytic plasma, ((1) inner electrode, (2) acrylic glass support, (3) outer electrode, (4) catalyst particles, (5) glass packing particles) [190].

due to its simplicity, the FBR is still frequently used to test various innovations, such as new catalysts or a new type of reactor heating.

2.3.2. *Fluidized bed reactor*

A fluidized bed reactor (FlBR) is a type of reactor in which catalyst particles are suspended in a gas flow. This causes the particles to behave as a fluidized bed with liquid-like properties (Fig. 11A1). The FLBR's configuration is essentially the same as the FBR's. The catalyst pellets are rest the grid through which the feed material passes. The only significant difference is in the processing conditions. While the catalyst remains on the grid during the reaction in the FBR, the FLBR's process conditions are selected so that the catalyst particles rise in the gas flow and become fluidized.

In the context of the CDM, FlBR have several advantages over FBRs. The most significant advantage is the ability to continuously extract the entrapped carbon product, which prevents the reactor from clogging [175,198–201]. Due to the generally higher gas flow rates, the FLBR exhibits improved mass and heat transfer [160]. At the same time, the FLBR can produce high-quality carbon materials, including MWCNTs [202,203].

Muradov investigated the possibility of using a FLBR for carbon dioxide removal in 2000 [204]. He designed, manufactured, and successfully tested a laboratory-scale FlBR for CDM with different carbon catalysts. After the experiments, the process was modeled theoretically, and it was concluded that this approach has great potential for large-scale implementation [205].

Keller et al. [206] used a FlBR with Fe_2O_3/Al_2O_3 as the catalyst for CDM. They found that the activity of the bed material for methane

cracking decreased linearly with the amount of carbon deposited on its surface. Once the carbon deposit amount reached 10 wt% of the catalyst mass, the particles lost mechanical integrity and the layer volume increased simultaneously, regardless of the reaction conditions.

Hadian et al. [207] conducted an experimental investigation of CDM kinetics in a FlBR. They found that, at lower reaction temperatures, more carbon was produced before complete deactivation, though the maximum reaction rate was lower. This was attributed to the catalyst's lower deactivation rate at lower temperatures. Similarly, the presence of hydrogen in the feed stream reduced the reaction rate but allowed for the production of greater amounts of carbon due to the catalyst's longer life. The carbon produced was mainly in the form of CNFs.

Parmar et al. [208] used a FlBR containing a 60% Ni-5% Cu-5% Zn/Al_2O_3 catalyst to produce CNTs. They separated the CNTs and partially regenerated the spent catalyst using ultrasonic treatment. They investigated the catalyst's regeneration capability by performing several reaction-regeneration cycles. After regeneration, the catalyst regained full activity, achieving a methane conversion of over 90% and producing high-quality CNTs (outer diameter: 60–80 nm; length: 5 μm).

The FLBR can be considered a further development of the FBR for implementing CDM on a pilot scale because it solves the main problem of clogging caused by carbon deposits. Several studies address catalyst stability, carbon deposition, and catalyst regeneration in FLBR under CDM reaction conditions.

Penilla et al. [209,210] investigated FLBR on a pilot scale for CDM. The authors used 150-μm $NiCu/Al_2O_3$ particles as a catalyst and selected the necessary fluidization conditions. They were able to achieve stable CNF production in a FLBR during the methane decomposition process using a Ni-based catalyst. By varying the process parameters, they demonstrated that raising the temperature increased hydrogen production but also accelerated catalyst deactivation. Increasing the GHSV resulted in a decrease in methane conversion and an increase in catalyst deactivation. At 700°C, the deposited carbon appeared mainly as long CNFs emerging from the nickel particles with a typical herringbone structure. The quality of the CNFs produced, as well as the reactor's overall performance, was quite competitive with the results obtained for the FBR. The reactor's capacity was sufficient to produce several hundred grams of CNFs per day.

Yang et al. [182] successfully applied FLBR using an Fe/Al_2O_3 catalyst at temperatures below 700°C, achieving hydrogen yields of over 80% and CNTs as the carbon product. They proposed a three-stage reactor process with catalyst regeneration. The first stage was the CDM process itself within the FLBR. The second stage involved separating the produced carbon and spent catalyst. In the third stage, the spent catalyst was regenerated and became suitable for reuse in the CDM process. The authors tested two methods for separating the catalyst from the produced carbon: vibro-separation and dense phase flotation. Vibro-separation yielded significantly better results and is considered more promising for future use.Dadsetan et al. [211] used microwave-heated FlBR with carbon pellets that served both as microwave receptor and catalyst. They achieved a constant methane conversion over 500 cumulative hours with a hydrogen selectivity of more than 90% at temperatures above 1000°C.

The CDM-FLBR reactor has also been the subject of theoretical calculations aimed at optimizing its operating conditions. One of the most recent studies is that of Tong et al. [212]. The authors developed a two-dimensional model of a Cu-based fluidized catalyst bed under CDM conditions with catalyst deactivation. Their calculations confirmed the experimental results that lower gas flow rates lead to higher conversion rates and greater catalyst stability.

2.3.3. Molten metal bubble column reactor (MMBCR)

Another solution to the problems of catalyst deactivation and reactor clogging caused by deposited carbon is to use a molten catalyst in a molten metal bubble column reactor (MMBCR). These catalysts were discussed in Section 2.2.3. Fig. 11B1 and Fig. 13B1 show an example of an MMBCR. The MMBCR design completely avoids catalyst deactivation caused by carbon deposition [156].

In the MMBCR, methane enters through a gas distributor at the bottom of the reactor, where it bubbles up through the liquid phase of the molten metal. Thermal decomposition of CH_4 occurs inside the bubbles and on their surfaces. Due to the significant density difference between carbon and liquid metal, solid carbon products floats on the liquid surface. This carbon can be removed from the surface of the molten metal by mechanical skimming. Carbon particles entrapped in the gas stream can be removed by cyclones, bag filters, or other solid-gas separation processes [213].

In the first MMBCR that was proposed and tested, the molten metal used had no catalytic activity. It only promoted the thermal decomposition of methane and the capture of carbon [214].

Many catalytically active metals, such as nickel (Ni), platinum (Pt), and palladium (Pd), cannot be used directly in the MMBCR due to their high melting points. However, this issue can be resolved by alloying these metals with those that melt at lower temperatures. For example, Upham et al. [148] successfully used a 27% Ni–73% Bi melt at 1065°C in a 1.1-m bubble column. Similarly, Chen et al. [95] reduced the operating temperature of a bismuth-cobalt alloy reactor from 1000°C to 800°C by adding molybdenum.

However, using more abundant metals may make MMBCR economically viable. For instance, Parkinson and Leal-Pérez [94,215] conducted independent techno-economic analyses of MMBCR and concluded that MMBCR technology could be competitive in the current market if the produced carbon is valorized and CO_2 emission taxes are sufficiently high.

Rahimi et al. [216] investigated a two-stage bubble column consisting of molten nickel-bismuth (NiBi) and molten bromide salt. Using an additional salt layer enables the production of pure carbon free of metallic impurities. Noh et al. [217] proposed and implemented a three-stage bubble column reactor for methane pyrolysis. In this reactor, solid ceramic beads are embedded in the liquid phase of the alloy catalyst, forming an additional mixed layer of solid ceramic beads and liquid metal on top of the pure liquid phase of the alloy catalyst. Compared to the two-stage system, the three-stage reactor with a bubble column exhibited higher methane conversion rates under gas flow conditions of 9 sccm and 985°C. In particular, a 6% increase in the methane conversion rate was observed.

MMBCR reactors have proven their ability to produce stable hydrogen and valuable carbon in the long term. However, there are also significant drawbacks that hinder their industrial use. These problems include low methane conversion, high energy requirements, and metal contamination of the produced carbon. Compared to other reactor types, these issues have slowed down industrial development [46].

2.3.4. Plasma reactor

The catalytic decomposition of methane also occurs in plasma, which requires specific reaction conditions and reactor design [54]. There are many different approaches to catalytic plasmas, and plasma technology uses electricity directly to carry out the reaction. In the next chapter, we will discuss the application of plasmas for CDM. Here, we will highlight some general information about plasma reactor design and types of plasma.

Plasma is an ionized gas consisting of electrons, ions, atoms (in the ground or excited state), molecules (in the ground or excited state), and free radicals. Regardless of the degree of ionization, the overall charge of the system is neutral. When an external electric field is applied, the neutral gas molecules in the plasma become excited, dissociated, and ionized. These particles then collide with each other and with the electrode surfaces, creating new charged particles.

Depending on whether the plasma particles are in thermal equilibrium with the surrounding medium, plasma can be divided into two types: equilibrium and non-equilibrium (Fig. 12B) [218]. Equilibrium plasma, also known as thermal or hot plasma, is fully ionized and has a

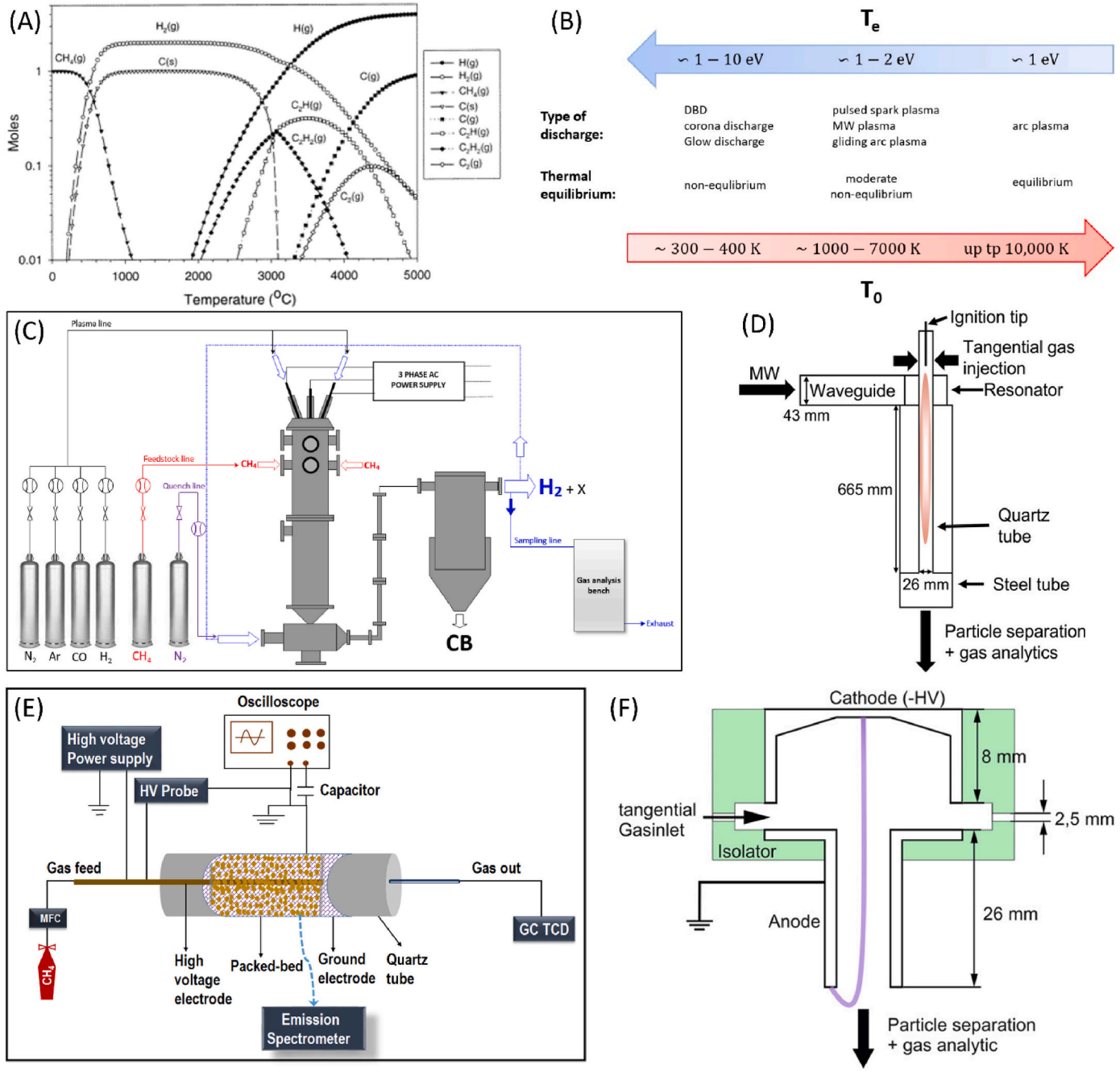

Fig. 12. (A) A simplified equilibrium diagram for decomposition products 1 mol methane (Reprinted with permission from Ref. [220]. Copyright 2002 American Chemical Society); (B) A brief summary of the main differences between the different plasma types, T_e is the electron energy, T_0 is the gas temperature (MDPI. Licence: CC BY 4.0) [56]; (C) Thermal plasma reactor [221]; (D) Gliding arc discharge reactor [222]; (E) DBD reactor [223]; (F) Microwave discharge reactor [222].

high temperature (>2000°C). Thermal plasmas require either high temperatures or high pressures. Non-equilibrium plasmas, also known as non-thermal plasmas, are not in thermal equilibrium; electrons have a much higher temperature than heavy particles [219]. Methane decomposition can occur in both thermal and non-thermal plasmas (Fig. 12A).

There are five types of plasma, each with a different reactor design, that can be used in CDM [54]: thermal plasma (Fig. 12C), corona discharge plasma, gliding arc plasma (Fig. 12D), dielectric barrier discharge plasma (Fig. 12E), and microwave discharge plasma (Fig. 12F).

We have already discussed thermal plasmas; the other types mentioned are non-thermal plasmas. Fig. 12B shows various plasma types. While the design of plasma reactors and operating conditions may vary, a detailed discussion of these topics is beyond the scope of this article.

3. Electrification of catalytic decomposition of methane

To produce hydrogen without emitting CO_2, the heat for the reaction must be generated without producing CO_2 emissions [97]. One solution is to use renewable energy sources. Electrifying the process enables the use of renewable solar and wind energy for methane processing, creating a CO_2-free cycle for hydrogen production from methane [38]. Apart from simple resistance heating, there are several more energy-efficient ways to supply electrical energy to the catalytic reaction. Electrification can significantly improve the economics of methane processing by

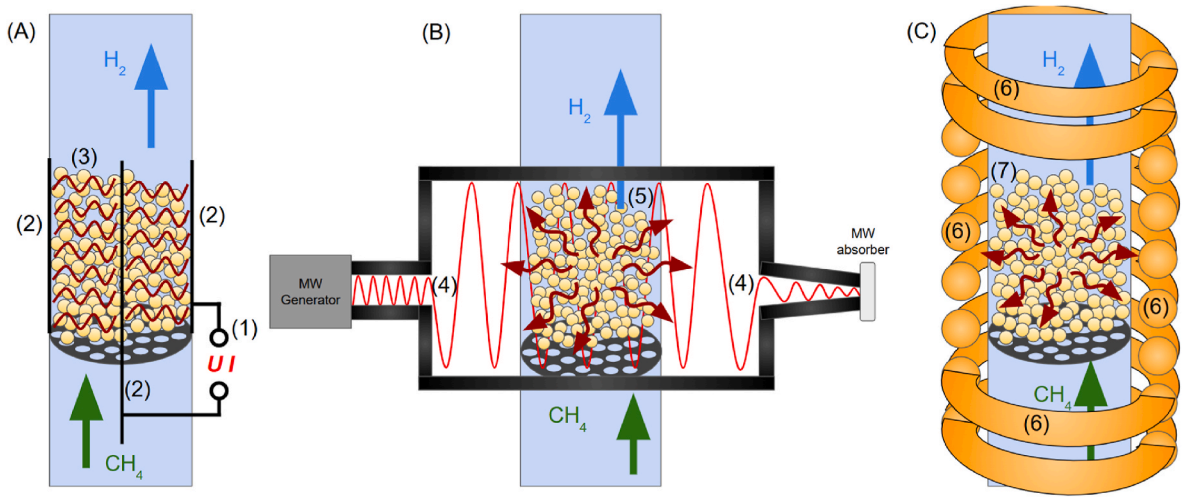

Fig. 13. (A) Schematic of the various electrified CDM reactors: (A) Plasma bed reactor; (B) Microwave-heated fluidized bed reactor; (C) Induction-heated fluidized bed reactor; (1) Power supply; (2) Cathodes for plasma generation; (3) Generated plasma in the catalyst layer; (4) Microwave radiation; (5) Microwave-heated fluidized bed; (6) Inductor; (7) Fluidized bed of magnetic nanoparticles heated by induction current.

using more energy-efficient equipment [224]. Electrification methods are not only alternatives to conventional heating techniques, they also represent a pathway toward decarbonizing hydrogen production and align with global energy transition goals. For a broader perspective on the electrification of catalytic systems, including reactor design, process intensification, and energy transfer strategies, we refer readers to some recent reviews on this topic [38,51].

In their review, Stankiewicz and Nigar [51] presented a comprehensive classification of possible methods for electrically driving chemical reactions. Of the approaches they proposed, three have been applied to CDM, according to the literature:

1) Plasma reactors (Fig. 13A)
2) Reactors with dielectric microwave heating (Fig. 13B)
3) Reactors with induction heating (Fig. 13C)

It is also worth noting the Joule-heating approach, which has gained attention as a means of electrifying catalytic processes. Although it has not yet been applied to catalytic methane decomposition, readers interested in this technique are referred to Zhen et al. [52]. The three CDM-relevant electrification approaches listed above are discussed in more detail in the following chapters.

3.1. Plasma

As previously mentioned, plasmas can be classified as either thermal or non-thermal. Non-thermal plasmas include gliding arc, microwave, and DBD plasmas. A more detailed classification is provided in the review by Nozaki et al. [53]. Table 2 lists some works dealing with the application of plasmas for the decomposition of methane into hydrogen and carbon. For readers seeking further insight into the broader role of plasma in hydrogen production, we recommend the recent comprehensive review by Wang et al. [54]. For a more CDM-focused perspective, the review by Wnukowski [56] offers an in-depth overview of plasma-based methane decomposition systems.

In addition to carbon-containing products and hydrogen, various radicals are formed during the plasma reaction, which may then recombine to form hydrocarbon species. Consequently, one of the main products of plasma pyrolysis of methane is often C_2H_2 [53]. The product selectivity shifts towards hydrogen and carbon as the temperature increases. Fincke et al. [220] performed calculations and demonstrated that solid CB and H_2 are the primary reaction products of plasma pyrolysis of methane within the operating temperature range of 1000–2500°C.

Fig. 11C shows the circuit diagram of a plasma reactor. Typically, the plasma generation system comprises an inner and an outer coaxial electrode, which are separated by a quartz tube through which the reaction gases are fed. The inner stainless steel electrode is located at the center of the reactor. The outer electrode, which is made of copper foil, is enclosed by the outside of the quartz tube. The tube itself can be empty for pure plasma, filled with a filler for packed plasma, or filled with a catalyst for catalytic plasma. The presence and composition of the filler affect the processes that take place in the plasma and can therefore influence the conversion of methane and the selectivity of different products.

Although thermal plasma has been successfully used in a number of

Table 2
Plasma applications for methane decomposition electrification.

Plasma type	Catalyst	Initial X_{CH_4} (%)	H_2 selectivity, %	Carbon morphology	year	Ref.
Thermal	–	99	95	CB	2023	[221]
Thermal	–	100	100	CB	2024	[225]
Thermal		100	100	Graphite	2024	[226]
Thermal	–	n.d	n.d.	CB	2005	[227]
Thermal		98	n.d.	Graphene	2023	[228]
Gliding arc		20	71	Graphite	2022	[222]
Gliding arc	–	58	95	n.d.	2018	[229]
Gliding arc		47	95	Graphite	2019	[230]
Microwave	–	64	87	CB	2022	[222]
Microwave		n.d.	n.d.	Graphite	2023	[231]
DBD	$NiO/\gamma\text{-}Al_2O_3$	6	27	CB	2022	[223]
DBD	–	49.6	52.6	CB	2024	[232]

studies for CDM [221,225,233], the main products of thermal plasma pyrolysis of methane are often heavier hydrocarbons rather than carbon [234]. Generally, reports on plasma technology suggest that thermal plasma is less suitable for commercial CDM use than non-thermal plasma due to its higher energy consumption [50,54].

Plasma technology uses electricity to directly carry out the reaction, making it directly relevant to CDM electrification. We will discuss its application in more detail in the next section.

In the context of CDM, thermal plasma is characterized by a higher conversion and reaction rates than non-thermal plasma. However, thermal plasma processes are much less selective than non-thermal processes due to the high operating temperature. Additionally, thermal plasma is much more energy-intensive, leading to significantly higher operating costs [54].

Fulcheri and Schwob [235] first proposed using thermal plasma to decompose methane into carbon and hydrogen in 1995. From 1997 to 2003, a plant operated in Karbomont, Canada. It produced hydrogen and CB from methane by plasma pyrolysis, with an annual production capacity of 20,000 tons of CB. However, the quality of the products was inadequate, leading to the plant's closure [236]. Attempts to produce hydrogen and carbon using thermal plasma are ongoing [221,225,237], but the prospects remain unclear.

Non-thermal plasmas have not found widespread industrial use. One reason for this is the scaling problem. Khalifeh et al. [190] investigated methane pyrolysis in a dielectric barrier discharge (DBD) reactor and found that methane decomposition stops at flow rates higher than 40 ml/min. Another reason is the low hydrogen production capacity. Kreuznacht et al. [222] compared gliding arc and microwave plasma discharges for CDM. The authors demonstrated that limitations in hydrogen production are associated with both methane conversion and H_2/C_2H_2 selectivity in both methods.

The main obstacles to using thermal plasma are the high temperatures and energy costs, which negate the advantages of electrification that plasma offers [50]. The main problem with using non-thermal plasmas is that the reaction products are primarily higher hydrocarbons, not hydrogen [238]. Compared to other CDM approaches, plasma pyrolysis has several advantages: ease of operation, high and stable methane conversion, lack of deactivation, and energy transfer without heat transfer. Due to these advantages, plasma methane pyrolysis has the highest TRL among all CDM methods for 2024 [14]. However, plasma reactors have significant disadvantages for CDM, including high energy consumption [229] and difficulty producing a carbon product more valuable than CB.

3.2. Microwave dielectric heating

Microwave heating works by using a dielectric material with high electrical susceptibility to absorb electromagnetic radio wave energy and convert it into thermal energy. As a non-contact heating method, microwave heating allows for the rapid, direct, and selective heating of the catalyst, preventing energy waste on heating the entire reactor [239]. For a broader overview of microwave-assisted heterogeneous catalysis and its applications across various catalytic systems, readers are referred to the comprehensive review by Palma et al. [57].

The choice of materials is crucial for microwave heating applications [52,57]. Conductors reflect microwaves and can be used in reactor walls to prevent radiation loss. Low-loss dielectrics are transparent to microwave radiation and should be used as windows through which radiation enters the reactor. Dielectric materials absorb microwave radiation and convert it into heat. Thus, dielectric materials should be used for the catalyst or heating element, if the catalyst is not already a heating element itself.

Microwave heating has been used successfully in several papers on CDM. Table 3 lists some of the successful results of CDM electrification by microwave heating.

Cooney and Xi [244] first used microwave heating for CDM in 1996.

Table 3
Results of using microwave heating in CDM.

Catalyst	Conditions T(°C)/GHSV ($L/g_{cat}/h$)	Initial X_{CH_4} (%)/ X_{CH_4} (%) at time (t)	Time (t) (hour)	Carbon morphology	Ref.
Carbon	917/0.4	98/5	500	CB	[211]
Ni–Fe-CNT	500/n.d.	40/12	2	n.d.	[240]
Carbon	800/0.16	95/29	2	CB, CNF	[241]
Ni–Cu-CNT	600/9	58/51	5	n.d.	[17]
NiFe/AC	800/1.8	51/43	1	CB	[242]
Ni/AC	800/1.8	66/71	1	CB, CNF	[242]
$SrTiNi_{0,08}O_3$/SiC	500/1.1	42/27	2	CNT	[243]

In an experimental comparison of conventional and microwave heating in a FBR containing a carbon catalyst, the authors found that microwave heating required temperatures 30–50°C lower than conventional heating to achieve the same methane conversion (18–53%). They attributed this result to the unique nature of the reaction triggered by microwaves. However, twenty years later, there is no evidence supporting the unique nature of microwave-heated reactions [52,245]. The most likely reason is the direct heating of the catalyst by microwaves and the different temperature distribution profile in the reactor.

As shown in Table 3, carbon-based materials are typically used as dielectric materials that absorb microwave energy in CDMs. However, SiC and alpha-alumina can also be used as microwave heating elements [246].

Dadestan et al. [211] demonstrated the feasibility of using microwave heating in conjunction with a FlBR. The authors used a carbon catalyst that achieved over 90% methane conversion after more than 500 h. Deibel et al. [243] obtained CNT-rich carbon on Ni-doped strontium titanate supported by microwave-heated ceramic materials. They hypothesized that combining microwave-heated production of high-value carbon with fluidized bed technology would accelerate the commercialization of CDM.

In summary, microwave heating offers a viable route for the electrification of CDM. Advantages include direct heating with low heat loss and low heat transfer limitations, the possibility of using electricity (including from renewable energy sources), the ability to produce CNTs, and the possibility of combining with FLBR. This set of advantages makes microwave heating an extremely promising way to electrify CDM.

3.3. Induction heating

Induction heating was only recently successfully tested for CDM. Essyed et al. [247] employed a carbon catalyst in an induction-heated methane decomposition process in a FBR. The process occurred at 900°C with a GHSV of 9.4 $L/g_{cat}/h$. The authors maintained a 61% methane conversion rate during the 7-h induction heating process. They demonstrated that valuable CNFs were produced during the reaction.

Although the authors used a FBR in previous work, there is no reason a FlBR could not be used instead. Induction heating in combination with FlBRs has already been used for other chemical processes [248–251].

In addition to induction heating used for CDM, there is a magnetic heating method that has not yet been tested but has similar requirements for the reactor [59]. Magnetic heating, which involves using magnetic nanoparticles as a heated element, is less common than induction heating. Magnetic heating is based on the idea that when magnetic particles are exposed to an alternating magnetic field, their magnetic moments respond to the field through hysteresis losses, generating heat. This causes the field to perform magnetic work, which is converted into heat [252].

Ceylan et al. [253] first demonstrated the possibility of using the superparamagnetic properties of nanoparticles to introduce thermal energy into a reactor. The authors successfully designed a FBR that was

heated by a magnetic induction coil and used Fe_3O_4/Fe_2O_3-based nanoparticles as the heating element. They also noted that, besides iron oxide, many other substances in nanoparticle form have magnetic properties and can be heated in the same way.

Magnetic heating was historically developed for liquid-phase processes [254], but there are examples of its application to gas-phase reactions. Meffre et al. [255] synthesized complex Fe@FeCo and Fe@Ru nanoparticles that possess superparamagnetic properties, that possess superparamagnetic properties enabling magnetic heating, and also exhibit catalytic activity for the Fischer–Tropsch synthesis. The obtained catalysts were successfully tested, proving the possibility of self-heating by magnetic heating.

Since then, a considerable number of papers have been published on using magnetically heated catalyst nanoparticles in various processes [58,256–260]. To the best of our knowledge, no studies have yet explored CDM over magnetically heated catalysts. Given that many CDM catalysts are nickel- and cobalt-based, using magnetic nanoparticles to heat this reaction is an extremely promising research topic. Recent reviews have comprehensively summarized the state of the art in magnetically heated catalytic systems and can serve as a valuable resource for further exploration [58,59].

In summary, the use of induction heating for CDM was investigated for the first time recently. Preliminary results are encouraging, and this type of heating has been successful in similar processes. No fundamental limitations have been identified so far, so this approach is considered very promising for CDM.

4. Conclusions

The co-production of hydrogen and carbon through CDM is a more economical and environmentally friendly approach than SMR and other conventional methods of hydrogen production. To create a CO/CO_2-free cycle for hydrogen production, reaction electrification is promising because it utilizes electricity from renewable/alternative energy sources that operate without CO/CO_2 emissions. One of the main differences between CDM and other methane-to-hydrogen conversion processes is the co-production of carbon. On the one hand, this contributes to the process's economic feasibility. On the other hand, it requires separating the solid product from the gas stream and enhancement of the catalyst's stability against carbon deposition. By using carbon materials as catalysts for CDM, the problems of separating the catalyst from the product can be avoided. However, deactivation of the catalyst due to carbon deposition on the catalyst surface and in the pores is a common problem. At the same time, there is a lack of work reporting the recovery of high-quality carbon in the CDM process over a carbon catalyst.

The most developed class of CDM catalysts is solid metal-based, including pure metals and metal alloy-based catalysts, both supported and bulk. The ability to fine-tune the structure of the catalysts' active phase allows for the production of high-quality, structured carbon species, such as MWCNTs, SWCNTs, CNFs, and graphene. However, depositing carbon on the catalyst surface can significantly decrease reaction conversion. Another challenge to successfully carrying outCDM using a solid metal-based catalyst is separating the catalyst from the carbon product to prevent leaching of the catalyst and contamination of the carbon by metal particles. With molten metal-based catalysts, however, it is unnecessary to separate the carbon product from the catalyst because the carbon can easily be separated from the molten metal's surface due to the difference in density. However, a liquid metal medium only offers limited opportunities for synthesizing structured carbon species.

The general classes of reactors for CDM can also be organized by the type of catalyst used. For solid catalysts, FBRs and FlBRs are primarily used. CDM with a molten metal catalyst is carried out in bubble column reactors. However, the reactor design for plasma catalysis generally involves heterogeneous processes on the surface of the solid catalyst. As a result, FBRs system with plasma-generating electrodes are most common.

Plasma catalysis and microwave catalysis are the most developed methods for electrification of the CDM reaction. Electrification of the CDM reaction is one of the ways to make it a commercially successful technology. Plasma technology is the most advanced technology for CDM and has even reached the stage of commercial utilization. Microwave heating has already successfully demonstrated its application for CDM. Although microwave heating requires a more complicated reactor design than conventional heating, the advantage of being able to directly heat the catalytic material or its support rapidly, uniformly, and selectively cannot be neglected. Microwave heating enables the recovery of various types of carbon, including CNTs. In addition, microwave heating enables the use of FlBRs. Induction heating for CDM has only recently been explored. However, given the success of this heating method in similar processes and the lack of fundamental limitations, it could also be promising for CDM.

CRediT authorship contribution statement

Sergey Girshevich: Writing – review & editing, Writing – original draft. **David Bajec:** Writing – review & editing, Funding acquisition. **Stanislav Yakushkin:** Writing – review & editing. **Janvit Teržan:** Writing – review & editing. **Blaž Likozar:** Writing – review & editing, Funding acquisition.

Funding

This work was supported by the European Research Council under the STORMING project (grant agreement no. 101069690), European Research Council under the e-CODUCT project (grant agreement no. 101058100), and Slovenian Research and Innovation Agency (post-doctoral project nr. Z2-50049). The project is also co-financed by the HyBreed project by Slovenian Research and Innovation Agency and the European Union – NextGenerationEU.

Declaration of competing interest

The authors declare the following financial interests/personal relationships which may be considered as potential competing interests: Blaz Likozar reports financial support was provided by European Research Council. David Bajec reports financial support was provided by Slovenian Research and Innovation Agency. Blaz Likozar reports financial support was provided by European Research Council. If there are other authors, they declare that they have no known competing financial interests or personal relationships that could have appeared to influence the work reported in this paper.

Acknowledgements

Special thanks go to the research and technical staff of the Department of Catalysis and Chemical Reaction Engineering at National Institute of Chemistry for their support and assistance throughout this review. The authors are also grateful for the funding that was provided by the European Research Council and Slovenian Research and Innovation Agency. The authors acknowledge partial support from the Republic of Slovenia, the Ministry of Higher Education, Science and Innovation, and the European Union – NextGenerationEU in the framework of the project HyBReED, part of the Slovenian Recovery and Resilience Plan. Views and opinions expressed are however those of the authors only and do not necessarily reflect those of the Republic of Slovenia, the Ministry of Higher Education, the European Union, or the European Commission. Neither the Republic of Slovenia, the Ministry of Higher Education, Science and Innovation, the European Union nor the European Commission can be held responsible for them.

References

[1] International Energy Agency. World energy outlook. 2024.
[2] Vacek Z, Vacek S, Cukor J. European forests under global climate change: review of tree growth processes, crises and management strategies. J Environ Manag 2023;332. https://doi.org/10.1016/j.jenvman.2023.117353.
[3] Gsottbauer E, Kirchler M, König-Kersting C. Financial professionals and climate experts have diverging perspectives on climate action. Commun Earth Environ 2024;5. https://doi.org/10.1038/s43247-024-01331-9.
[4] Lawrance EL, Thompson R, Newberry Le Vay J, Page L, Jennings N. The impact of climate change on mental health and emotional wellbeing: a narrative review of current evidence, and its implications. Int Rev Psychiatr 2022;34:443–98. https://doi.org/10.1080/09540261.2022.2128725.
[5] Evro S, Oni BA, Tomomewo OS. Carbon neutrality and hydrogen energy systems. Int J Hydrogen Energy 2024;78:1449–67. https://doi.org/10.1016/j.ijhydene.2024.06.407.
[6] Le TT, Sharma P, Bora BJ, Tran VD, Truong TH, Le HC, et al. Fueling the future: a comprehensive review of hydrogen energy systems and their challenges. Int J Hydrogen Energy 2024;54:791–816. https://doi.org/10.1016/j.ijhydene.2023.08.044.
[7] Xu X, Zhou Q, Yu D. The future of hydrogen energy: bio-hydrogen production technology. Int J Hydrogen Energy 2022;47:33677–98. https://doi.org/10.1016/j.ijhydene.2022.07.261.
[8] New hydrogen economy: hope or hype? World Energy Counc 2019:1–42.
[9] Fan Z, Weng W, Zhou J, Gu D, Xiao W. Catalytic decomposition of methane to produce hydrogen: a review. J Energy Chem 2021;58:415–30. https://doi.org/10.1016/j.jechem.2020.10.049.
[10] Franchi G, Capocelli M, De Falco M, Piemonte V, Barba D. Hydrogen production via steam reforming: a critical analysis of MR and RMM technologies. Membranes 2020;10. https://doi.org/10.3390/membranes10010010.
[11] Aramouni NAK, Touma JG, Tarboush BA, Zeaiter J, Ahmad MN. Catalyst design for dry reforming of methane: analysis review. Renew Sustain Energy Rev 2018;82:2570–85. https://doi.org/10.1016/j.rser.2017.09.076.
[12] Arku P, Regmi B, Dutta A. A review of catalytic partial oxidation of fossil fuels and biofuels: recent advances in catalyst development and kinetic modelling. Chem Eng Res Des 2018;136:385–402. https://doi.org/10.1016/j.cherd.2018.05.044.
[13] Alves L, Pereira V, Lagarteira T, Mendes A. Catalytic methane decomposition to boost the energy transition: scientific and technological advancements. Renew Sustain Energy Rev 2021;137. https://doi.org/10.1016/j.rser.2020.110465.
[14] International Energy Agency. Global hydrogen review 2024. Glob Hydrog Rev 2024 2024. https://doi.org/10.1787/cb2635f6-en.
[15] Karimi S, Bibak F, Meshkani F, Rastegarpanah A, Deng J, Liu Y, et al. Promotional roles of second metals in catalyzing methane decomposition over the Ni-based catalysts for hydrogen production: a critical review. Int J Hydrogen Energy 2021;46:20435–80. https://doi.org/10.1016/j.ijhydene.2021.03.160.
[16] Steinberg M. Fossil fuel decarbonization technology for mitigating global warming. 1999.
[17] Jiang C, Wang IW, Bai X, Balyan S, Robinson B, Hu J, et al. Methane catalytic pyrolysis by microwave and thermal heating over carbon nanotube-supported catalysts: productivity, kinetics, and energy efficiency. Ind Eng Chem Res 2022;61:5080–92. https://doi.org/10.1021/acs.iecr.1c05082.
[18] International Energy Agency. Global hydrogen review 2021. Paris: OECD Publishing; 2021.
[19] Keipi T, Tolvanen H, Konttinen J. Economic analysis of hydrogen production by methane thermal decomposition: comparison to competing technologies. Energy Convers Manag 2018;159:264–73. https://doi.org/10.1016/j.enconman.2017.12.063.
[20] Dufour J, Gálvez JL, Serrano DP, Moreno J, Martínez G. Life cycle assessment of hydrogen production by methane decomposition using carbonaceous catalysts. Int J Hydrogen Energy 2010;35:1205–12. https://doi.org/10.1016/j.ijhydene.2009.11.093.
[21] Dufour J, Serrano DP, Gálvez JL, González A, Soria E, Fierro JLG. Life cycle assessment of alternatives for hydrogen production from renewable and fossil sources. Int J Hydrogen Energy 2012;37:1173–83. https://doi.org/10.1016/j.ijhydene.2011.09.135.
[22] Riley J, Atallah C, Siriwardane R, Stevens R. Technoeconomic analysis for hydrogen and carbon Co-Production via catalytic pyrolysis of methane. Int J Hydrogen Energy 2021;46:20338–58. https://doi.org/10.1016/j.ijhydene.2021.03.151.
[23] Keipi T, Hankalin V, Nummelin J, Raiko R. Techno-economic analysis of four concepts for thermal decomposition of methane: reduction of CO2 emissions in natural gas combustion. Energy Convers Manag 2016;110:1–12. https://doi.org/10.1016/j.enconman.2015.11.057.
[24] Musamali R, Isa YM. Decomposition of methane to carbon and hydrogen: a catalytic perspective. Energy Technol 2019;7. https://doi.org/10.1002/ente.201800593.
[25] Hantoko D, Khan WU, Osman AI, Nasr M, Rashwan AK, Gambo Y, et al. Carbon–neutral hydrogen production by catalytic methane decomposition: a review. Springer International Publishing; 2024. https://doi.org/10.1007/s10311-024-01732-4.
[26] Qian JX, Chen TW, Enakonda LR, Liu D Bin, Basset JM, Zhou L. Methane decomposition to pure hydrogen and carbon nano materials: state-of-the-art and future perspectives. Int J Hydrogen Energy 2020;45:15721–43. https://doi.org/10.1016/j.ijhydene.2020.04.100.
[27] Ashik UPM, Wan Daud WMA, Abbas HF. Production of greenhouse gas free hydrogen by thermocatalytic decomposition of methane - a review. Renew Sustain Energy Rev 2015;44:221–56. https://doi.org/10.1016/j.rser.2014.12.025.
[28] Dufour J, Serrano DP, Gálvez JL, Moreno J, González A. Hydrogen production from fossil fuels: life cycle assessment of technologies with low greenhouse gas emissions. Energy Fuels 2011;25:2194–202. https://doi.org/10.1021/ef200124d.
[29] Li Y, Yu H, Jiang X, Deng G, Wen JZ, Tan Z. Techno-economic analysis for hydrogen-burning power plant with onsite hydrogen production unit based on methane catalytic decomposition. Energy Convers Manag 2023;277:116674. https://doi.org/10.1016/j.enconman.2023.116674.
[30] Zhang X, Kätelhön A, Sorda G, Helmin M, Rose M, Bardow A, et al. CO2 mitigation costs of catalytic methane decomposition. Energy 2018;151:826–38. https://doi.org/10.1016/j.energy.2018.03.132.
[31] Krasnikov DV, Bokova-Sirosh SN, Tsendsuren TO, Romanenko AI, Obraztsova ED, Volodin VA, et al. Influence of the growth temperature on the defective structure of the multi-walled carbon nanotubes. Phys Status Solidi Basic Res 2018;255:1–6. https://doi.org/10.1002/pssb.201700255.
[32] Rastegarpanah A, Rezaei M, Meshkani F, Zhang K, Zhao X, Pei W, et al. Mesoporous Ni/MeO x (Me = Al, Mg, Ti, and Si): highly efficient catalysts in the decomposition of methane for hydrogen production. Appl Surf Sci 2019;478:581–93. https://doi.org/10.1016/j.apsusc.2019.02.009.
[33] Torres D, Pinilla JL, Suelves I. Screening of Ni-Cu bimetallic catalysts for hydrogen and carbon nanofilaments production via catalytic decomposition of methane. Appl Catal Gen 2018;559:10–9. https://doi.org/10.1016/j.apcata.2018.04.011.
[34] Cao D, Li Y, Lv C, An Y, Song J, Li M, et al. Catalytic methane decomposition on in situ reduced FeCo alloy catalysts derived from layered double hydroxides. Nanomaterials 2024;14. https://doi.org/10.3390/nano14221831.
[35] Morshedy AS, El saied M, Awadallah AE, Mostafa MS. Ni@CaTiO3 nanocomposites for methane decomposition into hydrogen and multiwalled carbon nanotubes. ChemistrySelect 2024;9. https://doi.org/10.1002/slct.202401908.
[36] Dong Z, Li B, Cui C, Qian W, Jin Y, Wei F. Catalytic methane technology for carbon nanotubes and graphene. React Chem Eng 2020;5:991–1004. https://doi.org/10.1039/d0re00060d.
[37] Wismann ST, Engbæk JS, Vendelbo SB, Eriksen WL, Frandsen C, Mortensen PM, et al. Electrified methane reforming: elucidating transient phenomena. Chem Eng J 2021;425. https://doi.org/10.1016/j.cej.2021.131509.
[38] Kim YT, Lee JJ, Lee J. Electricity-driven reactors that promote thermochemical catalytic reactions via joule and induction heating. Chem Eng J 2023;470. https://doi.org/10.1016/j.cej.2023.144333.
[39] Wismann ST, Engbaek JS, Vendelbo SB, Bendixen FB, Eriksen WL, Aasberg-petersen K, et al. Electrified methane reforming: a compact approach to greener industrial hydrogen production. Science 2019;759(80):756–9.
[40] Keipi T, Tolvanen KES, Tolvanen H, Konttinen J. Thermo-catalytic decomposition of methane: the effect of reaction parameters on process design and the utilization possibilities of the produced carbon. Energy Convers Manag 2016;126:923–34. https://doi.org/10.1016/j.enconman.2016.08.060.
[41] Patlolla SR, Katsu K, Sharafian A, Wei K, Herrera OE, Mérida W. A review of methane pyrolysis technologies for hydrogen production. Renew Sustain Energy Rev 2023;181. https://doi.org/10.1016/j.rser.2023.113323.
[42] Hamdan M, Halawy L, Abdel Karim Aramouni N, Ahmad MN, Zeaiter J. Analytical review of the catalytic cracking of methane. Fuel 2022;324:124455. https://doi.org/10.1016/j.fuel.2022.124455.
[43] Qian JX, Chen TW, Enakonda LR, Liu D Bin, Mignani G, Basset JM, et al. Methane decomposition to produce COx-free hydrogen and nano-carbon over metal catalysts: a review. Int J Hydrogen Energy 2020;45:7981–8001. https://doi.org/10.1016/j.ijhydene.2020.01.052.
[44] Hamdani IR, Ahmad A, Chulliyil HM, Srinivasakannan C, Shoaibi AA, Hossain MM. Thermocatalytic decomposition of methane: a review on carbon-based catalysts. ACS Omega 2023;8:28945–67. https://doi.org/10.1021/acsomega.3c01936.
[45] Msheik M, Rodat S, Abanades S. Methane cracking for hydrogen production: a review of catalytic and molten media pyrolysis. Energies 2021;14. https://doi.org/10.3390/en14113107.
[46] Lang Z, Yanshaozuo Z, Shuang X, Ganming C, Huamei D. A mini-review on hydrogen and carbon production from methane pyrolysis by molten media. Energy Fuels 2024. https://doi.org/10.1021/acs.energyfuels.4c03860.
[47] Tong S, Miao B, Zhang L, Chan SH. Decarbonizing natural gas: a review of catalytic decomposition and carbon formation mechanisms. Energies 2022;15. https://doi.org/10.3390/en15072573.
[48] Välimäki E, Yli-Varo L, Romar H, Lassi U. Carbons formed in methane thermal and thermocatalytic decomposition processes: properties and applications. 7:50, https://doi.org/10.3390/c7030050; 2021.
[49] Sanyal A, Malalasekera W, Bandulasena H, Wijayantha KGU. Review of the production of turquoise hydrogen from methane catalytic decomposition: optimising reactors for Sustainable Hydrogen production. Int J Hydrogen Energy 2024;72:694–715. https://doi.org/10.1016/j.ijhydene.2024.05.397.
[50] Raza J, Khoja AH, Anwar M, Saleem F, Naqvi SR, Liaquat R, et al. Methane decomposition for hydrogen production: a comprehensive review on catalyst selection and reactor systems. Renew Sustain Energy Rev 2022;168:112774. https://doi.org/10.1016/j.rser.2022.112774.
[51] Stankiewicz AI, Nigar H. Beyond electrolysis: old challenges and new concepts of electricity-driven chemical reactors. React Chem Eng 2020;5:1005–16. https://doi.org/10.1039/d0re00116c.

[52] Zheng L, Ambrosetti M, Tronconi E. Joule-heated catalytic reactors toward decarbonization and process intensification: a review. ACS Eng Au 2024;4:4–21. https://doi.org/10.1021/acsengineeringau.3c00045.
[53] Nozaki T, Kim DY, Chen X. Plasma-enabled electrification of chemical processes toward decarbonization of society. Jpn J Appl Phys 2024;63. https://doi.org/10.35848/1347-4065/ad280f.
[54] Wang N, Otor HO, Rivera-Castro G, Hicks JC. Plasma catalysis for hydrogen production: a bright future for decarbonization. ACS Catal 2024;14:6749–98. https://doi.org/10.1021/acscatal.3c05434.
[55] Vander Wal R, Makiesse Nkiawete M. Carbons as catalysts in thermo-catalytic hydrocarbon decomposition: a review. 6:23, https://doi.org/10.3390/c6020023; 2020.
[56] Wnukowski M. Methane pyrolysis with the use of plasma: review of plasma reactors and process products. Energies 2023;16. https://doi.org/10.3390/en16186441.
[57] Palma V, Barba D, Cortese M, Martino M, Renda S, Meloni E. Microwaves and heterogeneous catalysis: a review on selected catalytic processes. Catalysts 2020;10. https://doi.org/10.3390/catal10020246.
[58] Wang W, Tuci G, Duong-Viet C, Liu Y, Rossin A, Luconi L, et al. Induction heating: an enabling technology for the heat management in catalytic processes. ACS Catal 2019;9:7921–35. https://doi.org/10.1021/acscatal.9b02471.
[59] Pavelić JS, Gyergyek S, Likozar B, Grilc M. Process electrification by magnetic heating of catalyst. Chem Eng J 2025;505. https://doi.org/10.1016/j.cej.2024.158928.
[60] Mirkarimi SMR, Bensaid S, Negro V, Chiaramonti D. Review of methane cracking over carbon-based catalyst for energy and fuels. Renew Sustain Energy Rev 2023;187:113747. https://doi.org/10.1016/j.rser.2023.113747.
[61] Dipu AL. Methane decomposition into COx-free hydrogen over a Ni-based catalyst: an overview. Int J Energy Res 2021;45:9858–77. https://doi.org/10.1002/er.6541.
[62] Pham CQ, Siang TJ, Kumar PS, Ahmad Z, Xiao L, Bahari MB, et al. Production of hydrogen and value-added carbon materials by catalytic methane decomposition: a review. Environ Chem Lett 2022;20:2339–59. https://doi.org/10.1007/s10311-022-01449-2.
[63] Weber RS, Xu M, Lopez-Ruiz JA, Jiang C, Hu J, Dagle RA. Toward rational design of nickel catalysts for thermocatalytic decomposition of methane for carbon dioxide-free hydrogen and value-added carbon Co-product: a review. ChemCatChem 2024;16. https://doi.org/10.1002/cctc.202301629.
[64] Zeza E, Pachatouridou E, Lappas AA, Iliopoulou EF. Cobalt decarbonization catalysts turning methane to clean hydrogen and valuable carbon nanostructures: a review. Catalysts 2025;15. https://doi.org/10.3390/catal15020145.
[65] Zhang K, Huang Z, Yang M, Liu M, Zhou Y, Zhan J, et al. Recent progress in melt pyrolysis: fabrication and applications of high-value carbon materials from abundant sources. SusMat 2023;3:558–80. https://doi.org/10.1002/sus2.157.
[66] McConnachie M, Konarova M, Smart S. Literature review of the catalytic pyrolysis of methane for hydrogen and carbon production. Int J Hydrogen Energy 2023. https://doi.org/10.1016/j.ijhydene.2023.03.123.
[67] Schützenberger LS P. Sur quelques faits relatifs à l'histoire du carbone. CR Acad Sci [Paris] 1890;111:774–8.
[68] Mondal KC, Ramesh Chandran S. Evaluation of the economic impact of hydrogen production by methane decomposition with steam reforming of methane process. Int J Hydrogen Energy 2014;39:9670–4. https://doi.org/10.1016/j.ijhydene.2014.04.087.
[69] Weger L, Abánades A, Butler T. Methane cracking as a bridge technology to the hydrogen economy. Int J Hydrogen Energy 2017;42:720–31. https://doi.org/10.1016/j.ijhydene.2016.11.029.
[70] Ahmed W, Awadallah AE, Aboul-Enein AA. Ni/CeO2–Al2O3 catalysts for methane thermo-catalytic decomposition to COx-free H2 production. Int J Hydrogen Energy 2016;41:18484–93. https://doi.org/10.1016/j.ijhydene.2016.08.177.
[71] Pudukudy M, Kadier A, Yaakob Z, Takriff MS. Non-oxidative thermocatalytic decomposition of methane into COx free hydrogen and nanocarbon over unsupported porous NiO and Fe2O3 catalysts. Int J Hydrogen Energy 2016;41:18509–21. https://doi.org/10.1016/j.ijhydene.2016.08.160.
[72] Ramasubramanian V, Ramsurn H, Price GL. Hydrogen production by catalytic decomposition of methane over Fe based bi-metallic catalysts supported on CeO2–ZrO2. Int J Hydrogen Energy 2020;45:12026–36. https://doi.org/10.1016/j.ijhydene.2020.02.170.
[73] Awadallah AE, Aboul-Enein AA, El-Desouki DS, Aboul-Gheit AK. Catalytic thermal decomposition of methane to CO x -free hydrogen and carbon nanotubes over MgO supported bimetallic group VIII catalysts. Appl Surf Sci 2014;296:100–7. https://doi.org/10.1016/j.apsusc.2014.01.055.
[74] Pudukudy M, Yaakob Z, Mazuki MZ, Takriff MS, Jahaya SS. One-pot sol-gel synthesis of MgO nanoparticles supported nickel and iron catalysts for undiluted methane decomposition into COx free hydrogen and nanocarbon. Appl Catal B Environ 2017;218:298–316. https://doi.org/10.1016/j.apcatb.2017.04.070.
[75] Deniz C, Karatepe N. Hydrogen and carbon nanotube production via catalytic decomposition of methane. Carbon Nanotub Graphene, Assoc Devices VI 2013;8814:881405. https://doi.org/10.1117/12.2023968.
[76] Bayat N, Rezaei M, Meshkani F. Methane decomposition over Ni-Fe/Al2O3 catalysts for production of COx-free hydrogen and carbon nanofiber. Int J Hydrogen Energy 2016;41:1574–84. https://doi.org/10.1016/j.ijhydene.2015.10.053.
[77] Saraswat SK, Pant KK. Synthesis of carbon nanotubes by thermo catalytic decomposition of methane over Cu and Zn promoted Ni/MCM-22 catalyst. J Environ Chem Eng 2013;1:746–54. https://doi.org/10.1016/j.jece.2013.07.009.
[78] Bayat N, Meshkani F, Rezaei M. Thermocatalytic decomposition of methane to COx-free hydrogen and carbon over Ni–Fe–Cu/Al2O3 catalysts. Int J Hydrogen Energy 2016;41:13039–49. https://doi.org/10.1016/j.ijhydene.2016.05.230.
[79] Ashik UPM, Wan DW, Hayashi J-I. A review on methane transformation to hydrogen and nanocarbon: relevance of catalyst characteristics and experimental parameters on yield. Renew Sustain Energy Rev 2017;76:743–67. https://doi.org/10.1016/j.rser.2017.03.088.
[80] Gao LZ, Kiwi-Minsker L, Renken A. Growth of carbon nanotubes and microfibers over stainless steel mesh by cracking of methane. Surf Coating Technol 2008;202:3029–42. https://doi.org/10.1016/j.surfcoat.2007.11.006.
[81] Snoeck JW, Froment GF, Fowles M. Filamentous carbon formation and gasification: thermodynamics, driving force, nucleation, and steady-state growth. J Catal 1997;169:240–9. https://doi.org/10.1006/jcat.1997.1634.
[82] Pinilla JL, Suelves I, Utrilla R, Gálvez ME, Lázaro MJ, Moliner R. Hydrogen production by thermo-catalytic decomposition of methane: regeneration of active carbons using CO2. J Power Sources 2007;169:103–9. https://doi.org/10.1016/j.jpowsour.2007.01.045.
[83] Liu F, Yang L, Song C. Chemical looping hydrogen production using activated carbon and carbon black as multi-function carriers. Int J Hydrogen Energy 2018;43:5501–11. https://doi.org/10.1016/j.ijhydene.2018.01.098.
[84] Wang C, Yang L, Liu F, Liu K, Zhang J. Sodium Carbonate-Modified activated carbon catalysts for enhanced hydrogen production via methane decomposition. Fuel 2025;382:133764. https://doi.org/10.1016/j.fuel.2024.133764.
[85] Zhang J, Li X, Xie W, Hao Q, Chen H, Ma X. Handy synthesis of robust Ni/carbon catalysts for methane decomposition by selective gasification of pine sawdust. Int J Hydrogen Energy 2018;43:19414–9. https://doi.org/10.1016/j.ijhydene.2018.08.207.
[86] Awadallah AE, Aboul-Enein AA, El-Desouki DS, Aboul-Gheit AK. Catalytic thermal decomposition of methane to CO x -free hydrogen and carbon nanotubes over MgO supported bimetallic group VIII catalysts. Appl Surf Sci 2014;296:100–7. https://doi.org/10.1016/j.apsusc.2014.01.055.
[87] Fakeeha AH, Ibrahim AA, Khan WU, Seshan K, Al Otaibi RL, Al-Fatesh AS. Hydrogen production via catalytic methane decomposition over alumina supported iron catalyst. Arab J Chem 2018;11:405–14. https://doi.org/10.1016/j.arabjc.2016.06.012.
[88] Alalga L, Benamar A, Trari M. Hydrogen production via methane decomposition over nickel supported on synthesized ZSM-5/MCM-41 zeolite composite material. Int J Hydrogen Energy 2021;46:28501–12. https://doi.org/10.1016/j.ijhydene.2021.06.090.
[89] Youn JR, Kim MJ, Kim KC, Kim M, Jung T, Go KS, et al. Highly efficient Co-added Ni/CeO2 catalyst for co-production of hydrogen and carbon nanotubes by methane decomposition. Fuel Process Technol 2024;263:108130. https://doi.org/10.1016/j.fuproc.2024.108130.
[90] Fakeeha AH, Kasim SO, Ibrahim AA, Al-Awadi AS, Alzahrani E, Abasaeed AE, et al. Methane decomposition over ZrO2-supported Fe and Fe–Ni catalysts—effects of doping La2O3 and WO3. Front Chem 2020;8:1–13. https://doi.org/10.3389/fchem.2020.00317.
[91] Bayazed MO, Al-Fatesh AS, Fakeeha AH, Ibrahim AA, Abasaeed AE, Alromaeh AI, et al. Role of MgO in Al2O3-supported Fe catalysts for hydrogen and carbon nanotubes formation during catalytic methane decomposition. Energy Sci Eng 2024:4166–79. https://doi.org/10.1002/ese3.1867.
[92] Awadallah AE, Aboul-Enein AA, Yonis MM, Aboul-Gheit AK. Effect of structural promoters on the catalytic performance of cobalt-based catalysts during natural gas decomposition to hydrogen and carbon nanotubes, 24; 2016. https://doi.org/10.1080/1536383X.2015.1132206.
[93] Khan WU, Hantoko D, Bakare IA, Al Shoaibi A, Chandrasekar S, Hossain MM. Co-Ni on zirconia and titania catalysts for methane decomposition to hydrogen and carbon nanomaterials: the role of metal-support interactions. Fuel 2024;369:131675. https://doi.org/10.1016/j.fuel.2024.131675.
[94] Leal Pérez BJ, Medrano Jiménez JA, Bhardwaj R, Goetheer E, van Sint Annaland M, Gallucci F. Methane pyrolysis in a molten gallium bubble column reactor for sustainable hydrogen production: proof of concept & techno-economic assessment. Int J Hydrogen Energy 2021;46:4917–35. https://doi.org/10.1016/j.ijhydene.2020.11.079.
[95] Chen L, Song Z, Zhang S, Chang CK, Chuang YC, Peng X, et al. Ternary NiMo-Bi liquid alloy catalyst for efficient hydrogen production from methane pyrolysis. Science (80-) 2023;381:857–61. https://doi.org/10.1126/science.adh8872.
[96] Ahmed S, Aitani A, Rahman F, Al-Dawood A, Al-Muhaish F. Decomposition of hydrocarbons to hydrogen and carbon. Appl Catal Gen 2009;359:1–24. https://doi.org/10.1016/j.apcata.2009.02.038.
[97] Perreault P, Boruntea C, Yadav HD, Soliño IP, Kummamuru NB. Combined methane pyrolysis and solid carbon gasification for electrified CO2-free hydrogen and syngas production. Energies 2023;16:7316.
[98] Yousefi M, Donne S. Technical challenges for developing thermal methane cracking in small or medium scales to produce pure hydrogen - a review. Int J Hydrogen Energy 2022;47:699–727. https://doi.org/10.1016/j.ijhydene.2021.10.100.
[99] Muradov NZ. CO2-free production of hydrogen by catalytic pyrolysis of hydrocarbon fuel. Energy Fuels 1998;12:41–8. https://doi.org/10.1021/ef9701145.
[100] Muradov N. Hydrogen via methane decomposition: an application for decarbonization of fossil fuels. Int J Hydrogen Energy 2001;26:1165–75. https://doi.org/10.1016/S0360-3199(01)00073-8.

[101] Muradov N. Emission-free fuel reformers for mobile and portable fuel cell applications. J Power Sources 2003;118:320–4. https://doi.org/10.1016/S0378-7753(03)00078-8.
[102] Muradov N. Catalysis of methane decomposition over elemental carbon. 2001.
[103] Stenina I, Yaroslavtsev A. Modern technologies of hydrogen production. Processes 2023;11. https://doi.org/10.3390/pr11010056.
[104] Muradov N, Smith F, T-Raissi A. Catalytic activity of carbons for methane decomposition reaction. Catal Today 2005;102–103:225–33. https://doi.org/10.1016/j.cattod.2005.02.018.
[105] Suelves I, Pinilla JL, Lázaro MJ, Moliner R. Carbonaceous materials as catalysts for decomposition of methane. Chem Eng J 2008;140:432–8. https://doi.org/10.1016/j.cej.2007.11.014.
[106] Yang L, Wu X, Liu F, Zhang X, He J, Saito K. Joint-use of activated carbon and carbon black to enhance catalytic stability during chemical looping methane decomposition process. Int J Hydrogen Energy 2020;45:13245–55. https://doi.org/10.1016/j.ijhydene.2020.03.055.
[107] Moliner R, Suelves I, Lázaro MJ, Moreno O. Thermocatalytic decomposition of methane over activated carbons: influence of textural properties and surface chemistry. Int J Hydrogen Energy 2005;30:293–300. https://doi.org/10.1016/j.ijhydene.2004.03.035.
[108] Suelves I, Lázaro MJ, Moliner R, Pinilla JL, Cubero H. Hydrogen production by methane decarbonization: carbonaceous catalysts. Int J Hydrogen Energy 2007;32:3320–6. https://doi.org/10.1016/j.ijhydene.2007.05.028.
[109] Zhang J, Li X, Chen H, Qi M, Zhang G, Hu H, et al. Hydrogen production by catalytic methane decomposition: carbon materials as catalysts or catalyst supports. Int J Hydrogen Energy 2017;42:19755–75. https://doi.org/10.1016/j.ijhydene.2017.06.197.
[110] Kameya Y, Hanamura K. Variation in catalytic activity of carbon black during methane decomposition: active site estimations from surface structural characteristics. Catal Lett 2012;142:460–3. https://doi.org/10.1007/s10562-012-0794-4.
[111] Wang J, Jin L, Zhou Y, Li Y, Hu H. Effect of Ca(NO3)2 addition in coal on properties of activated carbon for methane decomposition to hydrogen. Fuel Process Technol 2018;176:85–90. https://doi.org/10.1016/j.fuproc.2018.03.012.
[112] Zhang J, Qi M, Zhang G, Hu H, Xie L, Ma X. Co-production of hydrogen and fibrous carbons by methane decomposition using K2CO3/carbon hybrid as the catalyst. Int J Hydrogen Energy 2017;42:11047–52. https://doi.org/10.1016/j.ijhydene.2017.03.113.
[113] Tzeng SS, Hung KH, Ko TH. Growth of carbon nanofibers on activated carbon fiber fabrics. Carbon N Y 2006;44:859–65. https://doi.org/10.1016/j.carbon.2005.10.033.
[114] Slater WE. The influence of different surfaces on the decomposition of methane. J Chem Soc Trans 1916;109:160–4. https://doi.org/10.1039/CT9160900160.
[115] Li Y, Li D, Wang G. Methane decomposition to COx-free hydrogen and nano-carbon material on group 8-10 base metal catalysts: a review. Catal Today 2011;162:1–48. https://doi.org/10.1016/j.cattod.2010.12.042.
[116] Cheung CL, Kurtz A, Park H, Lieber CM. Diameter-controlled synthesis of carbon nanotubes. 2002. p. 2429–33.
[117] Liang W, Yan H, Chen C, Lin D, Tan K, Feng X, et al. Revealing the effect of nickel particle size on carbon formation type in the methane decomposition reaction. Catalysts 2020;10:1–20. https://doi.org/10.3390/catal10080890.
[118] Urdiana G, Valdez R, Lastra G, Valenzuela M, Olivas A. Production of hydrogen and carbon nanomaterials using transition metal catalysts through methane decomposition. Mater Lett 2018;217:9–12. https://doi.org/10.1016/j.matlet.2018.01.033.
[119] Bayat N, Rezaei M, Meshkani F. COx-free hydrogen and carbon nanofibers production by methane decomposition over nickel-alumina catalysts. Kor J Chem Eng 2016;33:490–9. https://doi.org/10.1007/s11814-015-0183-y.
[120] Tezel E, Figen HE, Baykara SZ. Hydrogen production by methane decomposition using bimetallic Ni–Fe catalysts. Int J Hydrogen Energy 2019;44:9930–40. https://doi.org/10.1016/j.ijhydene.2018.12.151.
[121] Torres D, De Llobet S, Pinilla JL, Lázaro MJ, Suelves I, Moliner R. Hydrogen production by catalytic decomposition of methane using a Fe-based catalyst in a fluidized bed reactor. J Nat Gas Chem 2012;21:367–73. https://doi.org/10.1016/S1003-9953(11)60378-2.
[122] Karaismailoğlu M, Figen HE, Baykara SZ. Methane decomposition over Fe-based catalysts. Int J Hydrogen Energy 2020;45:34773–82. https://doi.org/10.1016/j.ijhydene.2020.07.219.
[123] Chesnokov VV, Chichkan AS. Production of hydrogen by methane catalytic decomposition over Ni-Cu-Fe/Al2O3 catalyst. Int J Hydrogen Energy 2009;34:2979–85. https://doi.org/10.1016/j.ijhydene.2009.01.074.
[124] Hameed S, Comini E. Methane conversion for hydrogen production: technologies for a sustainable future. Sustain Energy Fuels 2024;8:670–83. https://doi.org/10.1039/d3se00972f.
[125] Abdel-Fattah E, Alotaibi MA, Alharthi AI. Thermo-catalytic methane decomposition over unsupported Fe–Al and Co–Al catalysts for hydrogen and carbon nanostructures production. Int J Hydrogen Energy 2024;64:685–94. https://doi.org/10.1016/j.ijhydene.2024.03.306.
[126] Qian J, Li H, Sun D, Shao W, Fan Q, Tao L, et al. Tuning Mg-Fe-O solid solutions towards optimized exsolution of active sites for thermal catalytic decomposition of methane. Chem Eng J 2024;497:154595. https://doi.org/10.1016/j.cej.2024.154595.
[127] Gao B, Wang IW, Ren L, Haines T, Hu J. Catalytic performance and reproducibility of Ni/Al2O3 and Co/Al2O3 mesoporous aerogel catalysts for methane decomposition. Ind Eng Chem Res 2019;58:798–807. https://doi.org/10.1021/acs.iecr.8b04223.
[128] Awadallah AE, Ahmed W, Noor El-Din MR, Aboul-Enein AA. Novel aluminosilicate hollow sphere as a catalyst support for methane decomposition to CO x -free hydrogen production. Appl Surf Sci 2013;287:415–22. https://doi.org/10.1016/j.apsusc.2013.09.173.
[129] Dasireddy VDBC, Likozar B. Activation and decomposition of methane over cobalt-, copper-, and iron-based heterogeneous catalysts for COx-free hydrogen and multiwalled carbon nanotube production. Energy Technol 2017;5:1344–55. https://doi.org/10.1002/ente.201600633.
[130] Silva RRCM, Oliveira HA, Guarino ACPF, Toledo BB, Moura MBT, Oliveira BTM, et al. Effect of support on methane decomposition for hydrogen production over cobalt catalysts. Int J Hydrogen Energy 2016;41:6763–72. https://doi.org/10.1016/j.ijhydene.2016.02.101.
[131] Al Mesfer MK, Danish M, Shah M. Synthesis, evaluation, and kinetic assessment of Co-based catalyst for enhanced methane decomposition reaction for hydrogen production. Int J Chem Kinet 2022;54:90–103. https://doi.org/10.1002/kin.21544.
[132] Fakeeha AH, Al-Fatesh AS, Chowdhury B, Ibrahim AA, Khan WU, Hassan S, et al. Bi-metallic catalysts of mesoporous Al2O3 supported on Fe, Ni and Mn for methane decomposition: effect of activation temperature. Chin J Chem Eng 2018;26:1904–11. https://doi.org/10.1016/j.cjche.2018.02.032.
[133] Torres D, Pinilla JL, Suelves I. Cobalt doping of α-Fe/Al2O3 catalysts for the production of hydrogen and high-quality carbon nanotubes by thermal decomposition of methane. Int J Hydrogen Energy 2020;45:19313–23. https://doi.org/10.1016/j.ijhydene.2020.05.104.
[134] Awadallah AE, Gad FK, Aboul-Enein AA, Labib MR, Aboul-Gheit AK. Direct conversion of natural gas into COx-free hydrogen and MWCNTs over commercial Ni–Mo/Al2O3 catalyst: effect of reaction parameters. Egypt J Pet 2013;22:27–34. https://doi.org/10.1016/j.ejpe.2012.11.012.
[135] Awadallah AE, Aboul-Enein AA, Aboul-Gheit AK. Various nickel doping in commercial Ni-Mo/Al2O3 as catalysts for natural gas decomposition to COx-free hydrogen production. Renew Energy 2013;57:671–8. https://doi.org/10.1016/j.renene.2013.02.024.
[136] Awadallah AE, Aboul-Enein AA, Aboul-Gheit AK. Impact of group VI metals addition to Co/MgO catalyst for non-oxidative decomposition of methane into COx-free hydrogen and carbon nanotubes. Fuel 2014;129:27–36. https://doi.org/10.1016/j.fuel.2014.03.038.
[137] Liang W, Yan H, Feng X, Chen C, Lin D, Liu J, et al. NiMgAlMo catalyst derived from a guest-host MoO42- mediated layered double hydroxide: high performance for the methane decomposition reaction. Appl Catal Gen 2020;597:117551. https://doi.org/10.1016/j.apcata.2020.117551.
[138] Rastegarpanah A, Rezaei M, Meshkani F, Zhang K, Zhao X, Pei W, et al. Influence of group VIB metals on activity of the Ni/MgO catalysts for methane decomposition. Appl Catal B Environ 2019;248:515–25. https://doi.org/10.1016/j.apcatb.2019.01.067.
[139] Wang D, Zhang J, Sun J, Gao W, Cui Y. Effect of metal additives on the catalytic performance of Ni/Al 2 O 3 catalyst in thermocatalytic decomposition of methane. Int J Hydrogen Energy 2019;44:7205–15. https://doi.org/10.1016/j.ijhydene.2019.01.272.
[140] Wu SL, Yang RX, Wey MY. Catalytic methane decomposition to hydrogen over a surface-protected core-shell Ni@SiO2 catalyst. Chem Eng Technol 2018;41:1448–56. https://doi.org/10.1002/ceat.201700315.
[141] Zhang C, Zhang W, Drewett NE, Wang X, Yoo SJ, Wang H, et al. Integrating catalysis of methane decomposition and electrocatalytic hydrogen evolution with Ni/CeO 2 for improved hydrogen production efficiency. ChemSusChem 2019;12:1000–10. https://doi.org/10.1002/cssc.201802618.
[142] Lázaro MJ, Echegoyen Y, Alegre C, Suelves I, Moliner R, Palacios JM. TiO2 as textural promoter on high loaded Ni catalysts for methane decomposition. Int J Hydrogen Energy 2008;33:3320–9. https://doi.org/10.1016/j.ijhydene.2008.03.050.
[143] Pudukudy M, Yaakob Z, Jia Q, Takriff MS. Catalytic decomposition of methane over rare earth metal (Ce and La) oxides supported iron catalysts. Appl Surf Sci 2019;467–468:236–48. https://doi.org/10.1016/j.apsusc.2018.10.122.
[144] Zhang X, Zhang M, Zhang J, Zhang Q, Tsubaki N, Tan Y, et al. Methane decomposition and carbon deposition over Ni/ZrO2 catalysts: comparison of amorphous, tetragonal, and monoclinic zirconia phase. Int J Hydrogen Energy 2019;44:17887–99. https://doi.org/10.1016/j.ijhydene.2019.05.174.
[145] Karaismailoglu M, Figen HE, Baykara SZ. Hydrogen production by catalytic methane decomposition over yttria doped nickel based catalysts. Int J Hydrogen Energy 2019;44:9922–9. https://doi.org/10.1016/j.ijhydene.2018.12.214.
[146] Sikander U, Samsudin MF, Sufian S, KuShaari KZ, Kait CF, Naqvi SR, et al. Tailored hydrotalcite-based Mg-Ni-Al catalyst for hydrogen production via methane decomposition: effect of nickel concentration and spinel-like structures. Int J Hydrogen Energy 2019;44:14424–33. https://doi.org/10.1016/j.ijhydene.2018.10.224.
[147] Calgaro CO, Perez-Lopez OW. Decomposition of methane over Co3−xAlxO4 (x=0–2) coprecipitated catalysts: the role of Co phases in the activity and stability. Int J Hydrogen Energy 2017;42:29756–72. https://doi.org/10.1016/j.ijhydene.2017.10.082.
[148] Upham DC, Agarwal V, Khechfe A, Snodgrass ZR, Gordon MJ, Metiu H, et al. Catalytic molten metals for the direct conversion of methane to hydrogen and separable carbon. 2017.
[149] Stoppel L, Fehling T, Geißler T, Baake E, Wetzel T. Carbon dioxide free production of hydrogen. IOP Conf Ser Mater Sci Eng 2017;228. https://doi.org/10.1088/1757-899X/228/1/012016. Institute of Physics Publishing.

[150] Wang K, Li WS, Zhou XP. Hydrogen generation by direct decomposition of hydrocarbons over molten magnesium. J Mol Catal Chem 2008;283:153–7. https://doi.org/10.1016/j.molcata.2007.12.018.
[151] Zeng J, Tarazkar M, Pennebaker T, Gordon MJ, Metiu H, McFarland EW. Catalytic methane pyrolysis with liquid and vapor phase tellurium. ACS Catal 2020;10:8223–30. https://doi.org/10.1021/acscatal.0c00805.
[152] Geißler T, Abánades A, Heinzel A, Mehravaran K, Müller G, Rathnam RK, et al. Hydrogen production via methane pyrolysis in a liquid metal bubble column reactor with a packed bed. Chem Eng J 2016;299:192–200. https://doi.org/10.1016/j.cej.2016.04.066.
[153] Palmer C, Tarazkar M, Kristoffersen HH, Gelinas J, Gordon MJ, McFarland EW, et al. Methane pyrolysis with a molten Cu-Bi alloy catalyst. ACS Catal 2019;9:8337–45. https://doi.org/10.1021/acscatal.9b01833.
[154] Hu X, Hu Y, Xu Q, Wang X, Li G, Cheng H, et al. Molten salt-promoted Ni–Fe/Al2O3 catalyst for methane decomposition. Int J Hydrogen Energy 2020;45:4244–53. https://doi.org/10.1016/j.ijhydene.2019.11.209.
[155] Palmer C, Tarazkar M, Gordon MJ, Metiu H, Mcfarland EW. Methane pyrolysis in low-cost, alkali-halide molten salts at high temperatures. Sustain Energy Fuels 2021;5:6107–23. https://doi.org/10.1039/d1se01408k.
[156] Kang D, Rahimi N, Gordon MJ, Metiu H, McFarland EW. Catalytic methane pyrolysis in molten MnCl2-KCl. Appl Catal B Environ 2019;254:659–66. https://doi.org/10.1016/j.apcatb.2019.05.026.
[157] Parkinson B, Patzschke CF, Nikolis D, Raman S, Dankworth DC, Hellgardt K. Methane pyrolysis in monovalent alkali halide salts: kinetics and pyrolytic carbon properties. Int J Hydrogen Energy 2021;46:6225–38. https://doi.org/10.1016/j.ijhydene.2020.11.150.
[158] Kang D, Palmer C, Mannini D, Rahimi N, Gordon MJ, Metiu H, et al. Catalytic methane pyrolysis in molten alkali chloride salts containing iron. ACS Catal 2020;10:7032–42. https://doi.org/10.1021/acscatal.0c01262.
[159] Kumar M. Carbon nanotube synthesis and growth mechanismIn. In: Siva Y, editor. Carbon nanotubes - synthesis, characterization, applications, intechopen limited-London. E-Publishing Inc; 2016. p. 147–70.
[160] Abbas HF, Wan Daud WMA. Hydrogen production by methane decomposition: a review. Int J Hydrogen Energy 2010;35:1160–90. https://doi.org/10.1016/j.ijhydene.2009.11.036.
[161] Naikoo GA, Arshad F, Hassan IU, Tabook MA, Pedram MZ, Mustaqeem M, et al. Thermocatalytic hydrogen production through decomposition of methane-A review. Front Chem 2021;9:1–24. https://doi.org/10.3389/fchem.2021.736801.
[162] Amin AM, Croiset E, Epling W. Review of methane catalytic cracking for hydrogen production. Int J Hydrogen Energy 2011;36:2904–35. https://doi.org/10.1016/j.ijhydene.2010.11.035.
[163] Takenaka S, Serizawa M, Otsuka K. Formation of filamentous carbons over supported Fe catalysts through methane decomposition. J Catal 2004;222:520–31. https://doi.org/10.1016/j.jcat.2003.11.017.
[164] Takenaka S, Ishida M, Serizawa M, Tanabe E, Otsuka K. Formation of carbon nanofibers and carbon nanotubes through methane decomposition over supported cobalt catalysts. J Phys Chem B 2004;108:11464–72. https://doi.org/10.1021/jp048827t.
[165] Torres D, Pinilla JL, Suelves I. Co-, cu-and fe-doped ni/al2o3 catalysts for the catalytic decomposition of methane into hydrogen and carbon nanofibers. Catalysts 2018;8. https://doi.org/10.3390/catal8080300.
[166] Avdeeva LB, Goncharova OV, Kochubey DI, Zaikovskii VI, Plyasova LM, Novgorodov BN, et al. Coprecipitated Ni-alumina and Ni-Cu-alumina catalysts of methane decomposition and carbon deposition. II. Evolution of the catalysts in reaction, 141. ELSEVIER; 1996.
[167] Ashik UPM, Wan Daud WMA. Probing the differential methane decomposition behaviors of n-Ni/SiO2, n-Fe/SiO2 and n-Co/SiO2 catalysts prepared by co-precipitation cum modified Stöber method. RSC Adv 2015;5:67227–41. https://doi.org/10.1039/c5ra10997c.
[168] Christensen KO, Chen D, Lødeng R, Holmen A. Effect of supports and Ni crystal size on carbon formation and sintering during steam methane reforming. Appl Catal Gen 2006;314:9–22. https://doi.org/10.1016/j.apcata.2006.07.028.
[169] Ayillath Kutteri D, Wang IW, Samanta A, Li L, Hu J. Methane decomposition to tip and base grown carbon nanotubes and COx-free H2 over mono- and bimetallic 3d transition metal catalysts. Catal Sci Technol 2018;8:858–69. https://doi.org/10.1039/c7cy01927k.
[170] Rahman MS, Croiset E, Hudgins RR. Catalytic decomposition of methane for hydrogen production. Top Catal 2006;37:137–45. https://doi.org/10.1007/s11244-006-0015-8.
[171] Fakeeha AH, Barama S, Ibrahim AA, Al-Otaibi RL, Barama A, Abasaeed AE, et al. In situ regeneration of alumina-supported Cobalt–iron catalysts for hydrogen production by catalytic methane decomposition. Catalysts 2018;8. https://doi.org/10.3390/catal8110567.
[172] Zhang T, Amiridis MD. Hydrogen production via the direct cracking of methane over silica-supported nickel catalysts. Appl Catal Gen 1998;167:161–72.
[173] Otsuka K, Takenaka S, Ohtsuki H. Production of pure hydrogen by cyclic decomposition of methane and oxidative elimination of carbon nanofibers on supported-Ni-based catalysts. Appl Catal Gen 2004;273:113–24. https://doi.org/10.1016/j.apcata.2004.06.021.
[174] Łamacz A. CNT and H2 production during CH4 decomposition over Ni/CeZrO2. I. A mechanistic study. ChemEngineering 2019;3:1–16. https://doi.org/10.3390/chemengineering3010026.
[175] Qian JX, Enakonda LR, Wang WJ, Gary D, Del-Gallo P, Basset JM, et al. Optimization of a fluidized bed reactor for methane decomposition over Fe/Al2O3 catalysts: activity and regeneration studies. Int J Hydrogen Energy 2019;44:31700–11. https://doi.org/10.1016/j.ijhydene.2019.10.058.
[176] Abbas HF, Daud WMAW. Thermocatalytic decomposition of methane for hydrogen production using activated carbon catalyst: regeneration and characterization studies. Int J Hydrogen Energy 2009;34:8034–45. https://doi.org/10.1016/j.ijhydene.2009.08.014.
[177] Aiello R, Fiscus JE, Zur Loye H-C, Amiridis MD. Hydrogen production via the direct cracking of methane over Ni/SiO 2 : catalyst deactivation and regeneration, 192; 2000.
[178] Chu Z, Zhao W, Xu D, Liu W, Han K, He Z, et al. The catalytic decomposition of CH4 using Ce-doped Fe/CaO-Ca12Al14O33 catalyst and its regeneration performance for H2 production. Sep Purif Technol 2025;355. https://doi.org/10.1016/j.seppur.2024.129670.
[179] Muradov NZ, Veziroğlu TN. From hydrocarbon to hydrogen-carbon to hydrogen economy. Int J Hydrogen Energy 2005;30:225–37. https://doi.org/10.1016/j.ijhydene.2004.03.033.
[180] Serban M, Lewis MA, Marshall CL, Doctor RD. Hydrogen production by direct contact pyrolysis of natural gas. Energy Fuels 2003;17:705–13. https://doi.org/10.1021/ef020271q.
[181] Hatanaka T, Yoda Y. Use of a swirling flow to mechanically regenerate catalysts after methane decomposition. Int J Hydrogen Energy 2022;47:20176–84. https://doi.org/10.1016/j.ijhydene.2022.04.138.
[182] Yang M, Baeyens J, Li S, Zhang H. Hydrogen and carbon produced by fluidized bed catalytic methane decomposition. Chem Eng Res Des 2024;204:67–80. https://doi.org/10.1016/j.cherd.2024.01.069.
[183] Keller M, Sharma A. Hydrogen production via methane cracking on dry-coated Fe/ZrO2with support recycle in a fluidized bed process. Energy Fuels 2021;35:847–55. https://doi.org/10.1021/acs.energyfuels.0c03287.
[184] Pathak S, McFarland E. Iron catalyzed methane pyrolysis in a stratified fluidized bed reactor. Energy Fuels 2024;38:12576–85. https://doi.org/10.1021/acs.energyfuels.4c01484.
[185] Wang IW, Kutteri DA, Gao B, Tian H, Hu J. Methane pyrolysis for carbon nanotubes and CO x -free H 2 over transition-metal catalysts. Energy Fuels 2019;33:197–205. https://doi.org/10.1021/acs.energyfuels.8b03502.
[186] Zhang J, Zou H, Qing Q, Yang Y, Li Q, Liu Z, et al. Effect of chemical oxidation on the gas sensing properties of multi-walled carbon nanotubes. Int J Nanotechnol 2009;6:735–44. https://doi.org/10.1504/IJNT.2009.025311.
[187] Datsyuk V, Kalyva M, Papagelis K, Parthenios J, Tasis D, Siokou A, et al. Chemical oxidation of multiwalled carbon nanotubes. Carbon N Y 2008;46:833–40. https://doi.org/10.1016/j.carbon.2008.02.012.
[188] Rosca ID, Watari F, Uo M, Akasaka T. Oxidation of multiwalled carbon nanotubes by nitric acid. Carbon N Y 2005;43:3124–31. https://doi.org/10.1016/j.carbon.2005.06.019.
[189] Eran TN, Guyot J, Boffito DC, Patience G. Kinetics, catalyst design, and hydrodynamic analysis in fischer-Tropsch synthesis: fixed bed vs fluidized bed reactors. Chem Eng J 2024;500:156796. https://doi.org/10.1016/j.cej.2024.156796.
[190] Khalifeh O, Taghvaei H, Mosallanejad A, Rahimpour MR, Shariati A. Extra pure hydrogen production through methane decomposition using nanosecond pulsed plasma and Pt-Re catalyst. Chem Eng J 2016;294:132–45. https://doi.org/10.1016/j.cej.2016.02.077.
[191] Carrillo AJ, Sastre D, Zazo L, Serrano DP, Coronado JM, Pizarro P. Hydrogen production by methane decomposition over MnOx/YSZ catalysts. Int J Hydrogen Energy 2016;41:19382–9. https://doi.org/10.1016/j.ijhydene.2016.04.138.
[192] Abanades S, Kimura H, Otsuka H. Hydrogen production from thermo-catalytic decomposition of methane using carbon black catalysts in an indirectly-irradiated tubular packed-bed solar reactor. Int J Hydrogen Energy 2014;39:18770–83. https://doi.org/10.1016/j.ijhydene.2014.09.058.
[193] Frusteri F, Italiano G, Espro C, Cannilla C, Bonura G. H 2 production by methane decomposition: catalytic and technological aspects. Int J Hydrogen Energy 2012;37:16367–74. https://doi.org/10.1016/j.ijhydene.2012.02.192.
[194] Lee SC, Seo HJ, Han GY. Hydrogen production by catalytic decomposition of methane over carbon black catalyst at high temperatures. Kor J Chem Eng 2013;30:1716–21. https://doi.org/10.1007/s11814-013-0107-7.
[195] Pinilla JL, Utrilla R, Karn RK, Suelves I, Lázaro MJ, Moliner R, et al. High temperature iron-based catalysts for hydrogen and nanostructured carbon production by methane decomposition. Int J Hydrogen Energy 2011;36:7832–43. https://doi.org/10.1016/j.ijhydene.2011.01.184.
[196] Konieczny A, Mondal K, Wiltowski T, Dydo P. Catalyst development for thermocatalytic decomposition of methane to hydrogen. Int J Hydrogen Energy 2008;33:264–72. https://doi.org/10.1016/j.ijhydene.2007.07.054.
[197] Abbas HF, Daud WMAW. Hydrogen production by thermocatalytic decomposition of methane using a fixed bed activated carbon in a pilot scale unit: apparent kinetic, deactivation and diffusional limitation studies. Int J Hydrogen Energy 2010;35:12268–76. https://doi.org/10.1016/j.ijhydene.2010.08.036.
[198] Ammendola P, Chirone R, Ruoppolo G, Russo G, Solimene R. Some issues in modelling methane catalytic decomposition in fluidized bed reactors. Int J Hydrogen Energy 2008;33:2679–94. https://doi.org/10.1016/j.ijhydene.2008.03.033.
[199] Łamacz A, Łabojko G. CNT and H2 production during CH4 decomposition over Ni/CeZrO2. II. catalyst performance and its regeneration in a fluidized bed. ChemEngineering 2019;3:1–18. https://doi.org/10.3390/chemengineering3010025.
[200] Jang WSC HT. Hydrogen production by the thermocatalytic decomposition of methane in a fluidized bed reactor. Kor J Chem Eng 2007;24:374–7.
[201] Lee KK, Han GY, Yoon KJ, Lee BK. Thermocatalytic hydrogen production from the methane in a fluidized bed with activated carbon catalyst. Catal Today 2004;93–95:81–6. https://doi.org/10.1016/j.cattod.2004.06.080.

[202] Allaedini G, Aminayi P, Tasirin SM. Methane decomposition for carbon nanotube production: optimization of the reaction parameters using response surface methodology. Chem Eng Res Des 2016;112:163–74. https://doi.org/10.1016/j.cherd.2016.06.010.
[203] Rashidi A, Lotfi R, Fakhrmosavi E, Zare M. Production of single-walled carbon nanotubes from methane over Co-Mo/MgO nanocatalyst: a comparative study of fixed and fluidized bed reactors. J Nat Gas Chem 2011;20:372–6. https://doi.org/10.1016/S1003-9953(10)60208-3.
[204] Martynov PN, Gulevich AV, Orlov YuI, Gulevsky VA. Water and hydrogen in heavy liquid metal coolant technology. Prog Nucl Energy 2005:1–14.
[205] Muradov N, Chen Z, Smith F. Fossil hydrogen with reduced CO2 emission: modeling thermocatalytic decomposition of methane in a fluidized bed of carbon particles. Int J Hydrogen Energy 2005;30:1149–58. https://doi.org/10.1016/j.ijhydene.2005.04.005.
[206] Keller M, Matsumura A, Sharma A. Spray-dried Fe/Al2O3 as a carbon carrier for COx-free hydrogen production via methane cracking in a fluidized bed process. Chem Eng J 2020;398:125612. https://doi.org/10.1016/j.cej.2020.125612.
[207] Hadian M, Marrevee DPF, Buist KA, Reesink BH, Bos ANR, van Bavel AP, et al. Kinetic study of thermocatalytic decomposition of methane over nickel supported catalyst in a fluidized bed reactor. Chem Eng Sci 2022;260:117938. https://doi.org/10.1016/j.ces.2022.117938.
[208] Parmar KR, Pant KK, Roy S. Blue hydrogen and carbon nanotube production via direct catalytic decomposition of methane in fluidized bed reactor: capture and extraction of carbon in the form of CNTs. Energy Convers Manag 2021;232:1–13. https://doi.org/10.1016/j.enconman.2021.113893.
[209] Pinilla JL, Lázaro MJ, Suelves I, Moliner R, Palacios JM. Characterization of nanofibrous carbon produced at pilot-scale in a fluidized bed reactor by methane decomposition. Chem Eng J 2010;156:170–6. https://doi.org/10.1016/j.cej.2009.10.032.
[210] Pinilla JL, Suelves I, Lázaro MJ, Moliner R, Palacios JM. Parametric study of the decomposition of methane using a NiCu/Al 2O3 catalyst in a fluidized bed reactor. Int J Hydrogen Energy 2010;35:9801–9. https://doi.org/10.1016/j.ijhydene.2009.10.008.
[211] Dadsetan M, Khan MF, Salakhi M, Bobicki ER, Thomson MJ. CO2-free hydrogen production via microwave-driven methane pyrolysis. Int J Hydrogen Energy 2023;48:14565–76. https://doi.org/10.1016/j.ijhydene.2022.12.353.
[212] Tong S, Miao B, Zhang W, Zhang L, Chan SH. Optimization of methane catalytic decomposition in a fluidized bed reactor: a computational approach. Energy Convers Manag 2023;297:117719. https://doi.org/10.1016/j.enconman.2023.117719.
[213] Le BT, Ngo SI, Il Lim Y, Do Lee U. One-dimensional kinetic model with novel bubble size equation in molten-metal bubble column reactors for CH4 pyrolysis. AIChE J 2024. https://doi.org/10.1002/aic.18540.
[214] Plevan M, Geißler T, Abánades A, Mehravaran K, Rathnam RK, Rubbia C, et al. Thermal cracking of methane in a liquid metal bubble column reactor: experiments and kinetic analysis. Int J Hydrogen Energy 2015;40:8020–33. https://doi.org/10.1016/j.ijhydene.2015.04.062.
[215] Parkinson B, Matthews JW, McConnaughy TB, Upham DC, McFarland EW. Techno-economic analysis of methane pyrolysis in molten metals: decarbonizing natural gas. Chem Eng Technol 2017;40:1022–30. https://doi.org/10.1002/ceat.201600414.
[216] Rahimi N, Kang D, Gelinas J, Menon A, Gordon MJ, Metiu H, et al. Solid carbon production and recovery from high temperature methane pyrolysis in bubble columns containing molten metals and molten salts. Carbon N Y 2019;151:181–91. https://doi.org/10.1016/j.carbon.2019.05.041.
[217] Noh YG, Lee YJ, Kim J, Kim YK, Ha JS, Kalanur SS, et al. Enhanced efficiency in CO2-free hydrogen production from methane in a molten liquid alloy bubble column reactor with zirconia beads. Chem Eng J 2021;428:131095. https://doi.org/10.1016/j.cej.2021.131095.
[218] Tendero C, Tixier C, Tristant P, Desmaison J, Leprince P. Atmospheric pressure plasmas: a review. Spectrochim Acta Part B At Spectrosc 2006;61:2–30. https://doi.org/10.1016/j.sab.2005.10.003.
[219] Foest R, Schmidt M, Becker K. Microplasmas, an emerging field of low-temperature plasma science and technology. Int J Mass Spectrom 2006;248:87–102. https://doi.org/10.1016/j.ijms.2005.11.010.
[220] Fincke JR, Anderson RP, Hyde TA, Detering BA. Plasma pyrolysis of methane to hydrogen and carbon black. Ind Eng Chem Res 2002;41:1425–35. https://doi.org/10.1021/ie010722e.
[221] Fulcheri L, Rohani VJ, Wyse E, Hardman N, Dames E. An energy-efficient plasma methane pyrolysis process for high yields of carbon black and hydrogen. Int J Hydrogen Energy 2023;48:2920–8. https://doi.org/10.1016/j.ijhydene.2022.10.144.
[222] Kreuznacht S, Purcel M, Böddeker S, Awakowicz P, Xia W, Muhler M, et al. Comparison of the performance of a microwave plasma torch and a gliding arc plasma for hydrogen production via methane pyrolysis. Plasma Process Polym 2023;20. https://doi.org/10.1002/ppap.202200132.
[223] Chawdhury P, Bhanudas Rawool S, Umamaheswara Rao M, Subrahmanyam C. Methane decomposition by plasma-packed bed non-thermal plasma reactor. Chem Eng Sci 2022;258:117779. https://doi.org/10.1016/j.ces.2022.117779.
[224] Lašič Jurković D, Puliyalil H, Pohar A, Likozar B. Plasma-activated methane partial oxidation reaction to oxygenate platform chemicals over Fe, Mo, Pd and zeolite catalysts. Int J Energy Res 2019;43:8085–99. https://doi.org/10.1002/er.4806.
[225] Daghagheleh O, Schenk J, Zarl MA, Lehner M, Farkas M, Zheng H. Feasibility of a plasma furnace for methane pyrolysis: hydrogen and carbon production. Energies 2024;17. https://doi.org/10.3390/en17010167.
[226] Daghagheleh O, Schenk J, Zheng H, Zarl MA, Farkas M, Ernst D, et al. Optimizing methane plasma pyrolysis for instant hydrogen and high-quality carbon production. Int J Hydrogen Energy 2024;79:1406–17. https://doi.org/10.1016/j.ijhydene.2024.07.129.
[227] Kim KS, Seo JH, Nam JS, Ju WT, Hong SH. Production of hydrogen and carbon black by methane decomposition using DC-RF hybrid thermal plasmas. IEEE Trans Plasma Sci 2005;33:813–23. https://doi.org/10.1109/TPS.2005.844526.
[228] Mahmoud R, Gitzhofer F, Blanchard J, Abatzoglou N. In situ graphene synthesis study in inductively coupled radiofrequency thermal plasma reactor using methane precursor. Plasma Chem Plasma Process 2024;44:65–94. https://doi.org/10.1007/s11090-023-10408-w.
[229] Moshrefi MM, Rashidi F. Hydrogen production from methane decomposition in cold plasma reactor with rotating electrodes. Plasma Chem Plasma Process 2018;38:503–15. https://doi.org/10.1007/s11090-018-9875-5.
[230] Kheirollahivash M, Rashidi F, Moshrefi MM. Hydrogen production from methane decomposition using a mobile and elongating arc plasma reactor. Plasma Chem Plasma Process 2019;39:445–59. https://doi.org/10.1007/s11090-018-9950-y.
[231] Dadsetan M, Latham KG, Khan MF, Zaher MH, Manzoor S, Bobicki ER, et al. Characterization of carbon products from microwave-driven methane pyrolysis. Carbon Trends 2023;12:100277. https://doi.org/10.1016/j.cartre.2023.100277.
[232] Wang S, Wang J, Feng D, Wang F, Zhao Y, Sun S. Plasma-induced methane catalytic cracking: effects of experimental conditions. Int J Hydrogen Energy 2024;63:284–93. https://doi.org/10.1016/j.ijhydene.2024.03.178.
[233] Chen G, Tu X, Homm G, Weidenkaff A. Plasma pyrolysis for a sustainable hydrogen economy. Nat Rev Mater 2022;7:333–4. https://doi.org/10.1038/s41578-022-00439-8.
[234] Lee YH, Oh JH, Choi S. Evaluation of process conditions for methane pyrolysis applying the triple thermal plasma system. Int J Hydrogen Energy 2023;48:27127–36. https://doi.org/10.1016/j.ijhydene.2023.03.427.
[235] Fulcheri L, Schwob Y. From methane to hydrogen, carbon black and water. Int J Hydrogen Energy 1995;20:197–202. https://doi.org/10.1016/0360-3199(94)E0022-Q.
[236] Schneider S, Bajohr S, Graf F, Kolb T. State of the art of hydrogen production via pyrolysis of natural gas. ChemBioEng Rev 2020;7:150–8. https://doi.org/10.1002/cben.202000014.
[237] Gautier M, Rohani V, Fulcheri L. Direct decarbonization of methane by thermal plasma for the production of hydrogen and high value-added carbon black. Int J Hydrogen Energy 2017;42:28140–56. https://doi.org/10.1016/j.ijhydene.2017.09.021.
[238] Tsai CH, Chen KT. Production of hydrogen and nano carbon powders from direct plasmalysis of methane. Int J Hydrogen Energy 2009;34:833–8. https://doi.org/10.1016/j.ijhydene.2008.10.061.
[239] Goyal H, Chen TY, Chen W, Vlachos DG. A review of microwave-assisted process intensified multiphase reactors. Chem Eng J 2022;430:133183. https://doi.org/10.1016/j.cej.2021.133183.
[240] Jiang C, Araia A, Balyan S, Robinson B, Brown S, Caiola A, et al. Kinetic study of Ni-M/CNT catalyst in methane decomposition under microwave irradiation. Appl Catal B Environ 2024;340. https://doi.org/10.1016/j.apcatb.2023.123255.
[241] Domínguez A, Fidalgo B, Fernández Y, Pis JJ, Menéndez JA. Microwave-assisted catalytic decomposition of methane over activated carbon for CO2-free hydrogen production. Int J Hydrogen Energy 2007;32:4792–9. https://doi.org/10.1016/j.ijhydene.2007.07.041.
[242] Ellison C, Lauterbach J, Smith MW. Activated carbon supported Ni, Fe, and bimetallic NiFe catalysts for COx-free H2 production by microwave methane pyrolysis. Int J Hydrogen Energy 2024;55:1062–70. https://doi.org/10.1016/j.ijhydene.2023.11.150.
[243] Deibel A, Balyan S, Zhu X, Jiang C, Li W, Hu J, et al. Surface exsolving perovskite ceramics as catalyst for microwave methane pyrolysis to co-generate hydrogen and carbon nanotube. Int J Hydrogen Energy 2024;69:874–82. https://doi.org/10.1016/j.ijhydene.2024.05.052.
[244] Cooney DO, Xi Z. Production of hydrogen from methane and methane/steam in a microwave irradiated char-loaded reactor. Fuel Sci Technol Int 1996;14:1111–41. https://doi.org/10.1080/08843759608947631.
[245] Kappe CO, Pieber B, Dallinger D. Microwave effects in organic synthesis: myth or reality? Angew Chem Int Ed 2013;52:1088–94. https://doi.org/10.1002/anie.201204103.
[246] Thomas JR, Fucher F. Thermal modeling of microwave heated packed and fluidized bed catalytic reactors. J Microw Power Electromagn Energy 2000;35:165–74. https://doi.org/10.1080/08327823.2000.11688433.
[247] Essyed A, Pham XH, Truong-Phuoc L, Romero T, Nhut JM, Duong-Viet C, et al. High-efficiency graphene-coated macroscopic composite for catalytic methane decomposition operated with induction heating. Chem Eng J 2024;485:150006. https://doi.org/10.1016/j.cej.2024.150006.
[248] Yan Y, Li N, Pan Y, Shi L, Xie G, Liu Z, et al. Hydrogen-rich syngas production from tobacco stem pyrolysis in an electromagnetic induction heating fluidized bed reactor. Int J Hydrogen Energy 2024;68:1271–80. https://doi.org/10.1016/j.ijhydene.2024.04.344.
[249] Idakiev VV, Bück A, Tsotsas E, Mörl L. Model-based studies on the heat transfer in an inductively heated fluidized bed. Chem-Ing-Tech 2016;88:656–65. https://doi.org/10.1002/cite.201500074.
[250] Idakiev VV, Marx S, Roßau A, Bück A, Tsotsas E, Mörl L. Inductive heating of fluidized beds: influence on fluidization behavior. Powder Technol 2015;286:90–7. https://doi.org/10.1016/j.powtec.2015.08.003.
[251] Latifi M. A novel fluidized and induction heated microreactor for catalyst testing. AIChE J 2014;60:3107–22.

[252] Rosensweig RE. Heating magnetic fluid with alternating magnetic field. J Magn Magn Mater 2002;252:370–4. https://doi.org/10.1016/S0304-8853(02)00706-0.
[253] Ceylan S, Friese C, Lammel C, Mazac K, Kirschning A. Inductive heating for organic synthesis by using functionalized magnetic nanoparticles inside microreactors. Angew Chem Int Ed 2008;47:8950–3. https://doi.org/10.1002/anie.200801474.
[254] Chaudhuri SR, Hartwig J, Kupracz L, Kodanek T, Wegner J, Kirschning A. Oxidations of allylic and benzylic alcohols under inductively-heated flow conditions with gold-doped superparamagnetic nanostructured particles as catalyst and oxygen as oxidant. Adv Synth Catal 2014;356:3530–8. https://doi.org/10.1002/adsc.201400261.
[255] Meffre A, Mehdaoui B, Connord V, Carrey J, Fazzini PF, Lachaize S, et al. Complex nano-objects displaying both magnetic and catalytic properties: a proof of concept for magnetically induced heterogeneous catalysis. Nano Lett 2015;15:3241–8. https://doi.org/10.1021/acs.nanolett.5b00446.
[256] Niether C, Faure S, Bordet A, Deseure J, Chatenet M, Carrey J, et al. Improved water electrolysis using magnetic heating of FeC-Ni core-shell nanoparticles. Nat Energy 2018;3:476–83. https://doi.org/10.1038/s41560-018-0132-1.
[257] Bordet A, Lacroix LM, Fazzini PF, Carrey J, Soulantica K, Chaudret B. Magnetically induced continuous CO2Hydrogenation using composite iron carbide nanoparticles of exceptionally high heating power. Angew Chem Int Ed 2016;55:15894–8. https://doi.org/10.1002/anie.201609477.
[258] Gyergyek S, Kocjan A, Grilc M, Likozar B, Hočevar B, Makovec D. A hierarchical Ru-bearing alumina/magnetic iron-oxide composite for the magnetically heated hydrogenation of furfural. Green Chem 2020;22:5978–83. https://doi.org/10.1039/d0gc00966k.
[259] Gyergyek S, Chernyshova E, Bőőr K, Nečemer M, Makovec D. Magnetic carbon nanocomposites via the graphitization of glucose and their induction heating. J Alloys Compd 2023;953. https://doi.org/10.1016/j.jallcom.2023.170139.
[260] Ponikvar Ž, Sedminek A, Teržan J, Skubic L, Lavrič Ž, Huš M, et al. Electrified dynamically responsive ammonia decomposition to hydrogen based on magnetic heating of a Ru nanocatalyst. ChemSusChem 2024:1–11. https://doi.org/10.1002/cssc.202401970. 202401970.